

Numerical assessment of a hybrid approach for simulating three-dimensional flow and advective transport in fractured rocks

Chuen-Fa Ni, Ph.D., P.E.

Professor & Director

**Center for Environmental Studies, National Central University
Graduate Institute of Applied Geology, National Central University**



國立中央大學 環境研究中心
Center for Environmental Studies

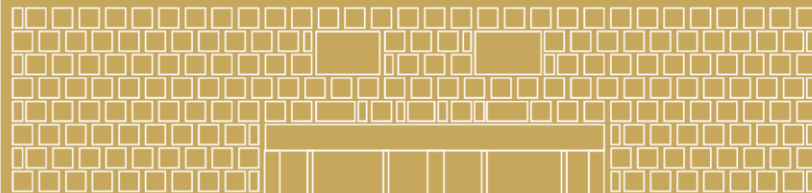


Quote:

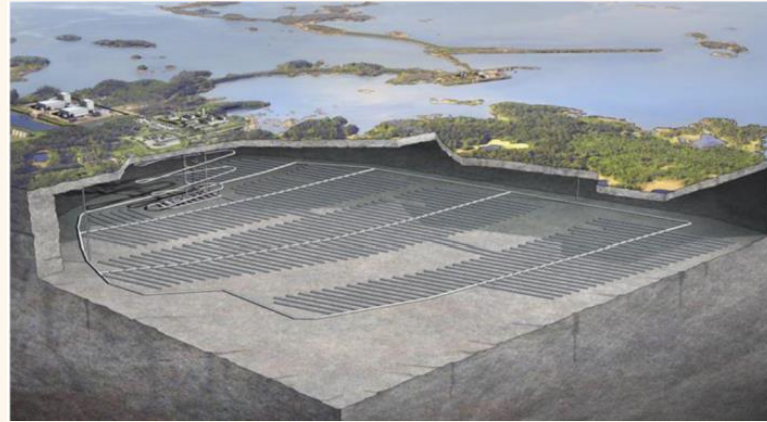
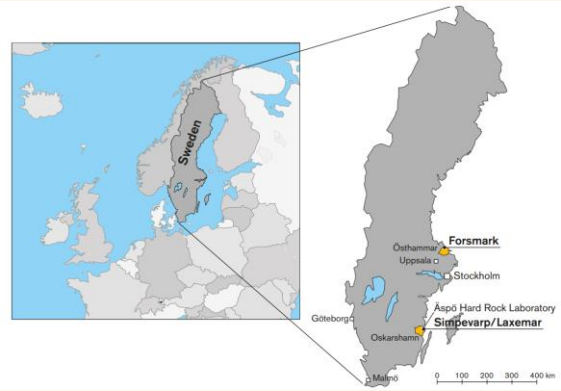
In God we trust, all others must bring data.

If you don't know how to ask the right question, you discover nothing.

-- William Edward Deming (October 14, 1900 – December 20¹, 1993)

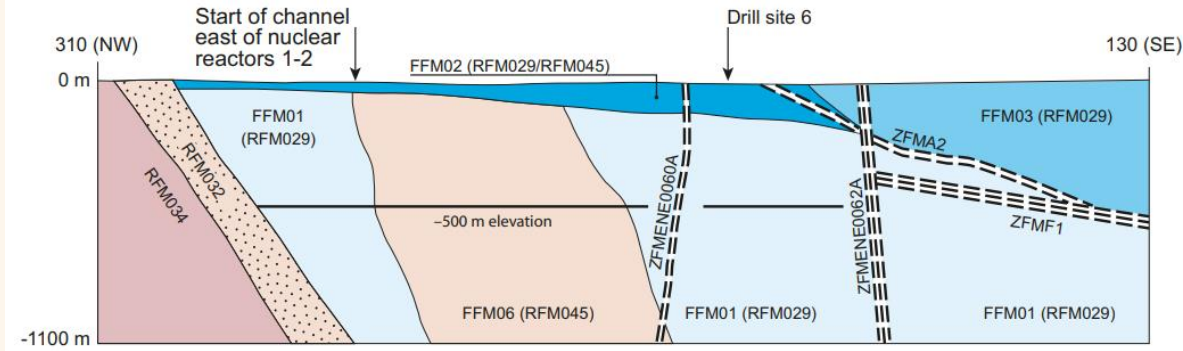


Key issues

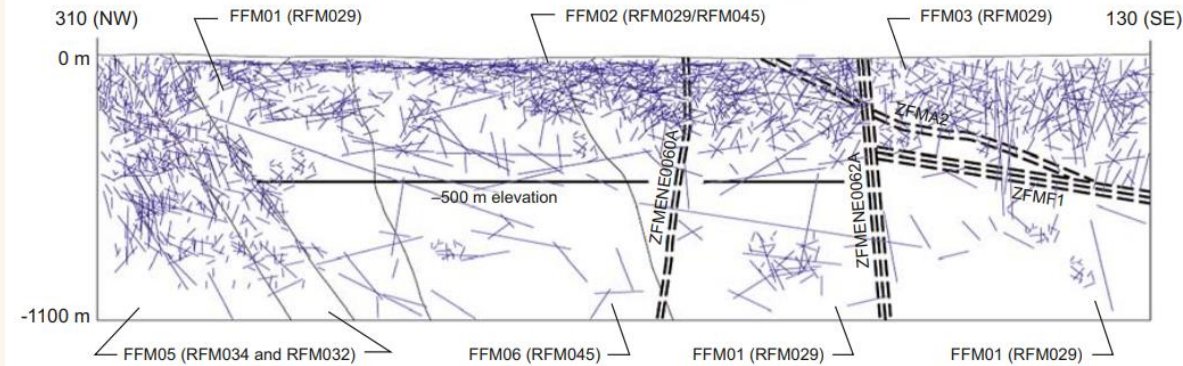


(Andersson, 2020)

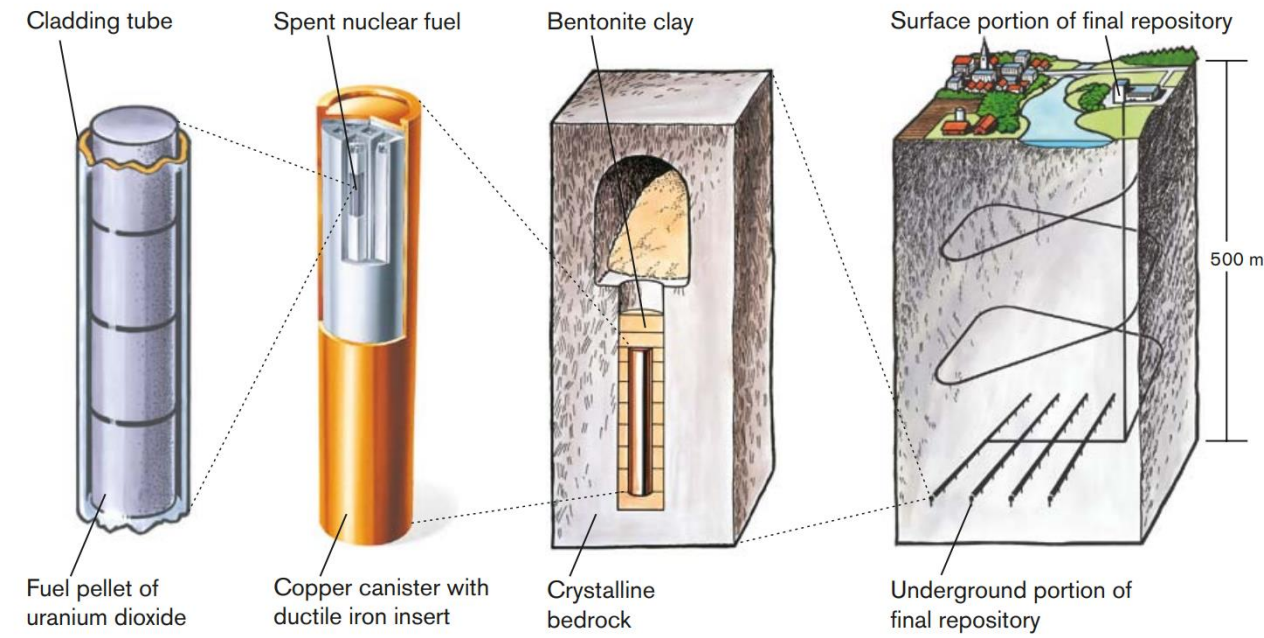
Conceptual fracture domain model



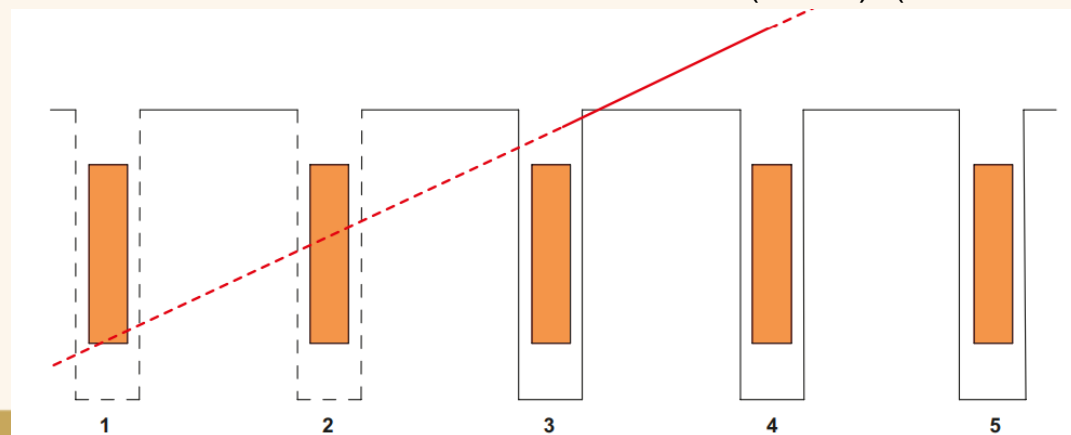
Conceptual hydrogeological DFN model (connected open fractures)



The KBS-3 concept for disposal of spent nuclear fuel (SKB, 2011)



Fractures are not allowed to intersect deposition holes in accordance with the Extended Full Perimeter Intersection Criterion (EFPC). (Munier 2006)



Challenge with scale interactions

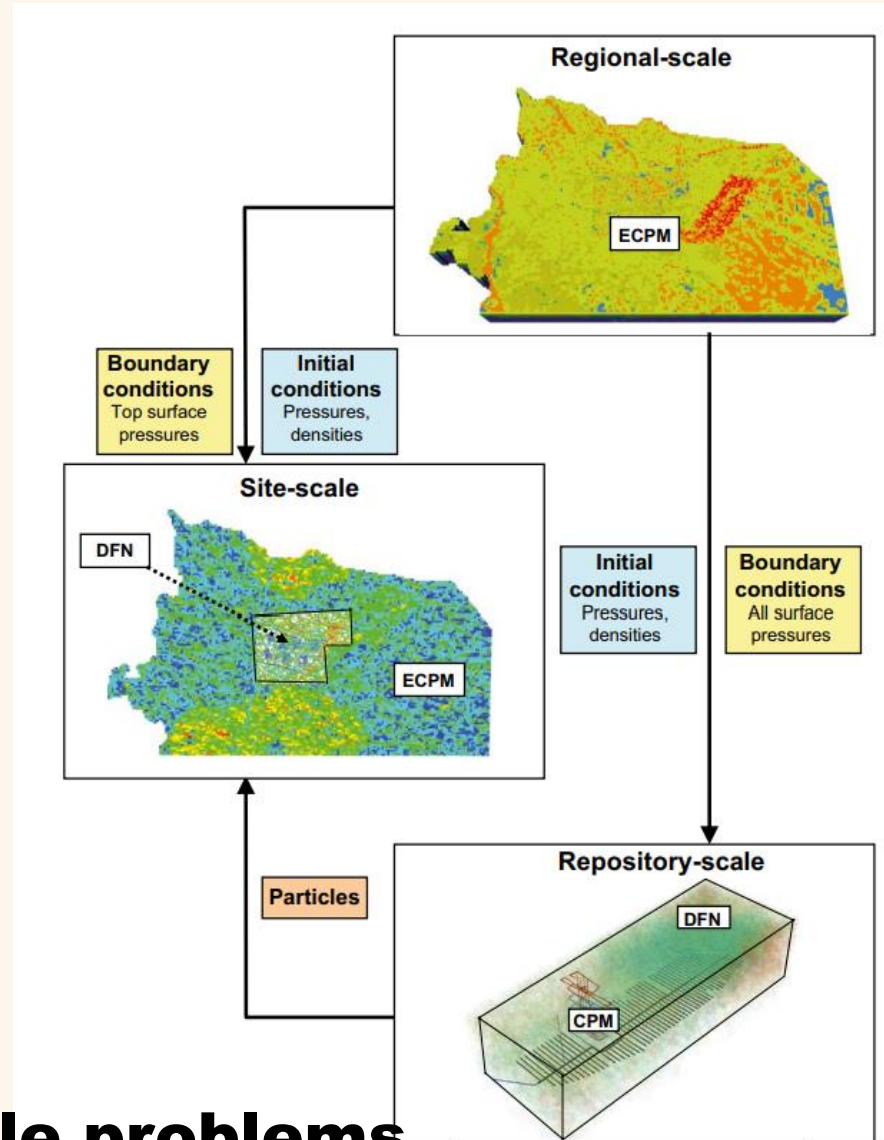
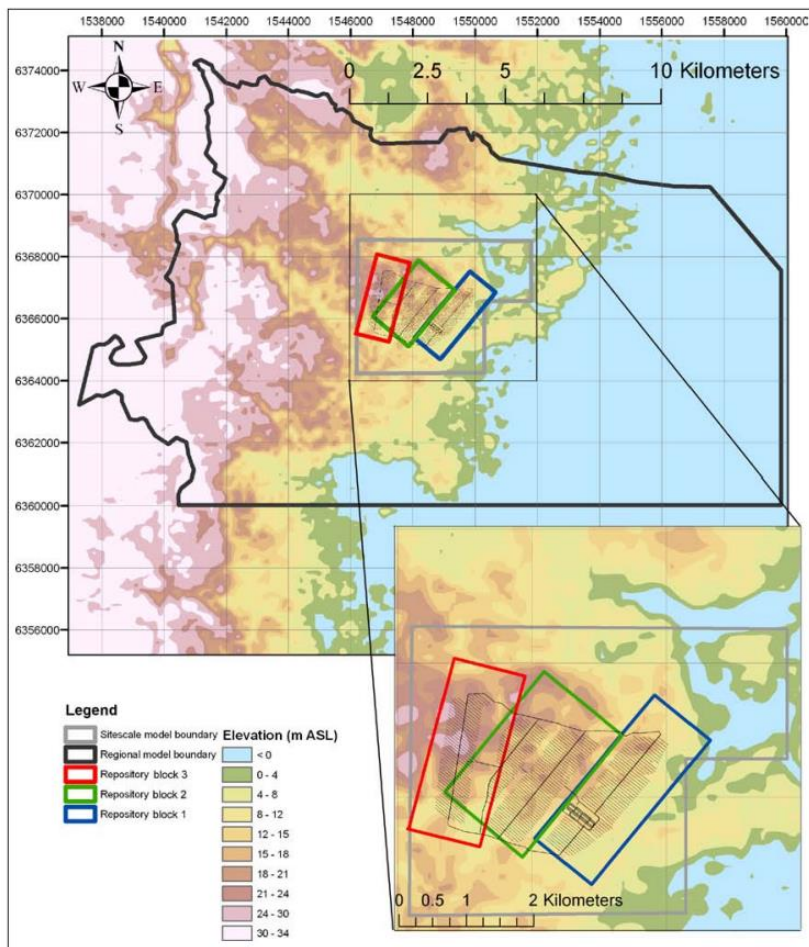


Figure 3-10. Illustration of the concepts of model scales, embedding, and the transfer of data between scales. Models are defined by hydraulic conductivity (CPM/ECPM) or transmissivity (DFN).

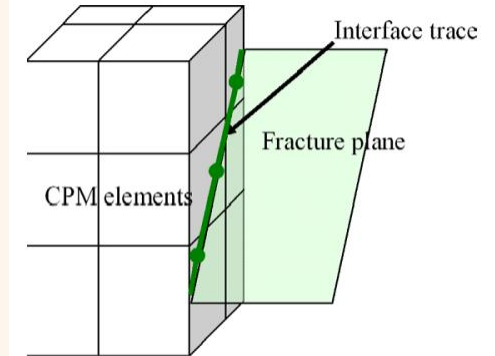


Figure 3-6. Illustration of embedding between DFN and CPM sub-models. A finite-element CPM mesh is shown on the left. The right hand surface is intersected by a single fracture plane. Extra equations are used to link the DFN to the CPM.

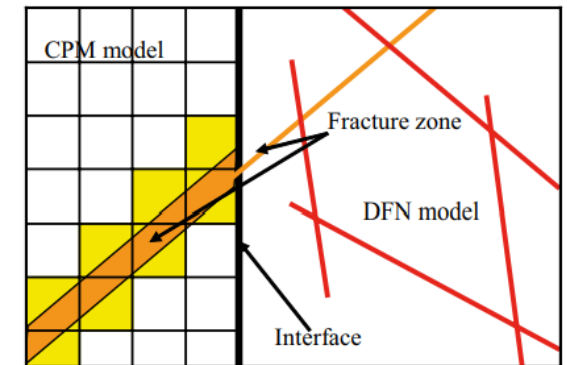


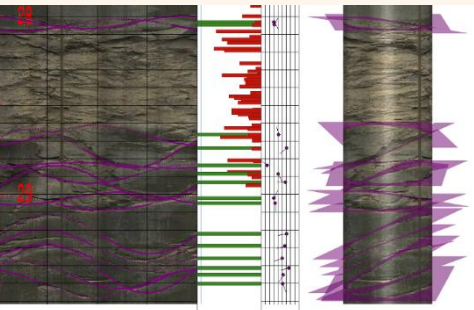
Figure 3-18. Schematic illustration of continuity of DZs across a CPM/DFN interface in a ConnectFlow model. The DFN region is to the right with a CPM grid to the left.

**Models for multiple scale problems.
From fractures to regional-scales**

(Joyce et al., 2010)

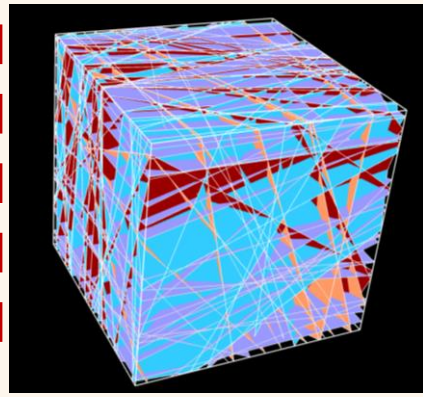
Flow & reactive transport modeling

Our previous approach!



Input data

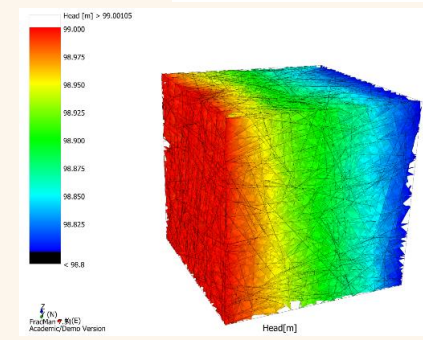
Fracture data analysis



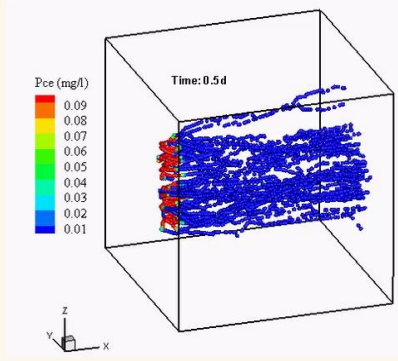
Generation of DFN

Mesh generation

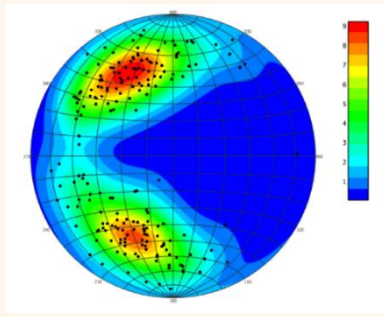
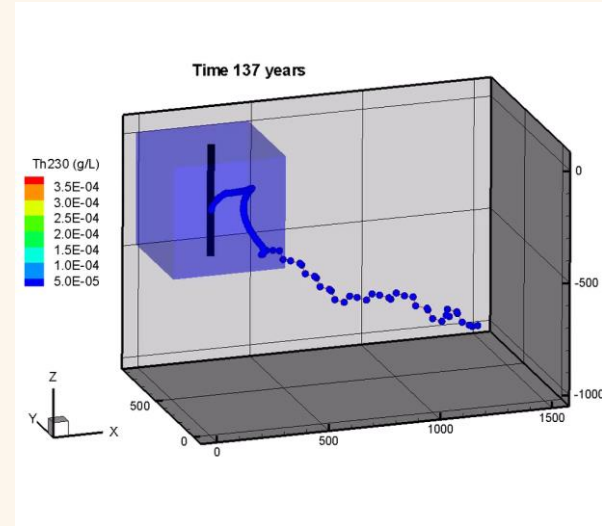
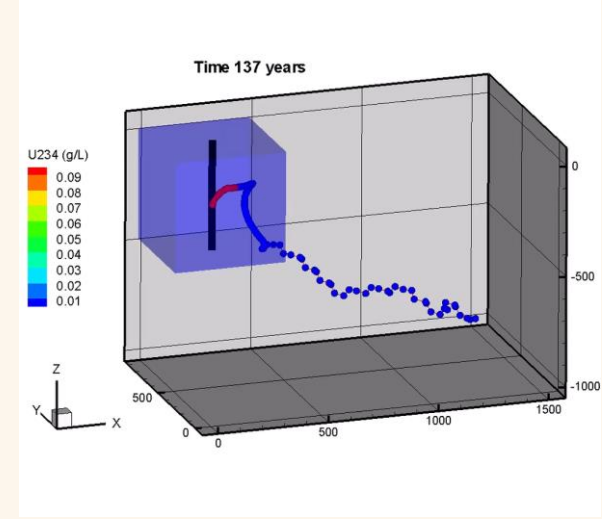
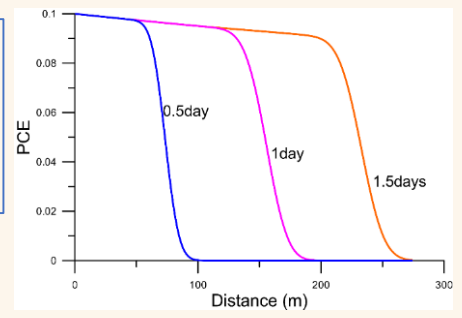
Flow simulation



Particle tracking



Chemical reaction (*PCE degradation*) & solute transport



Selroos et al., 2016

(Vu et al., 2019)

Objectives

- **Develop a DFN & ECPM (Hybrid-domain) model for simulating flow and advective transport in fractured rock systems.**

First phase: Flow and advective transport

- **Evaluate potential releasing pathways for radionuclides to leave the canisters, i.e., Q1 to Q3 paths.**

Test case

Numerical model – the concept

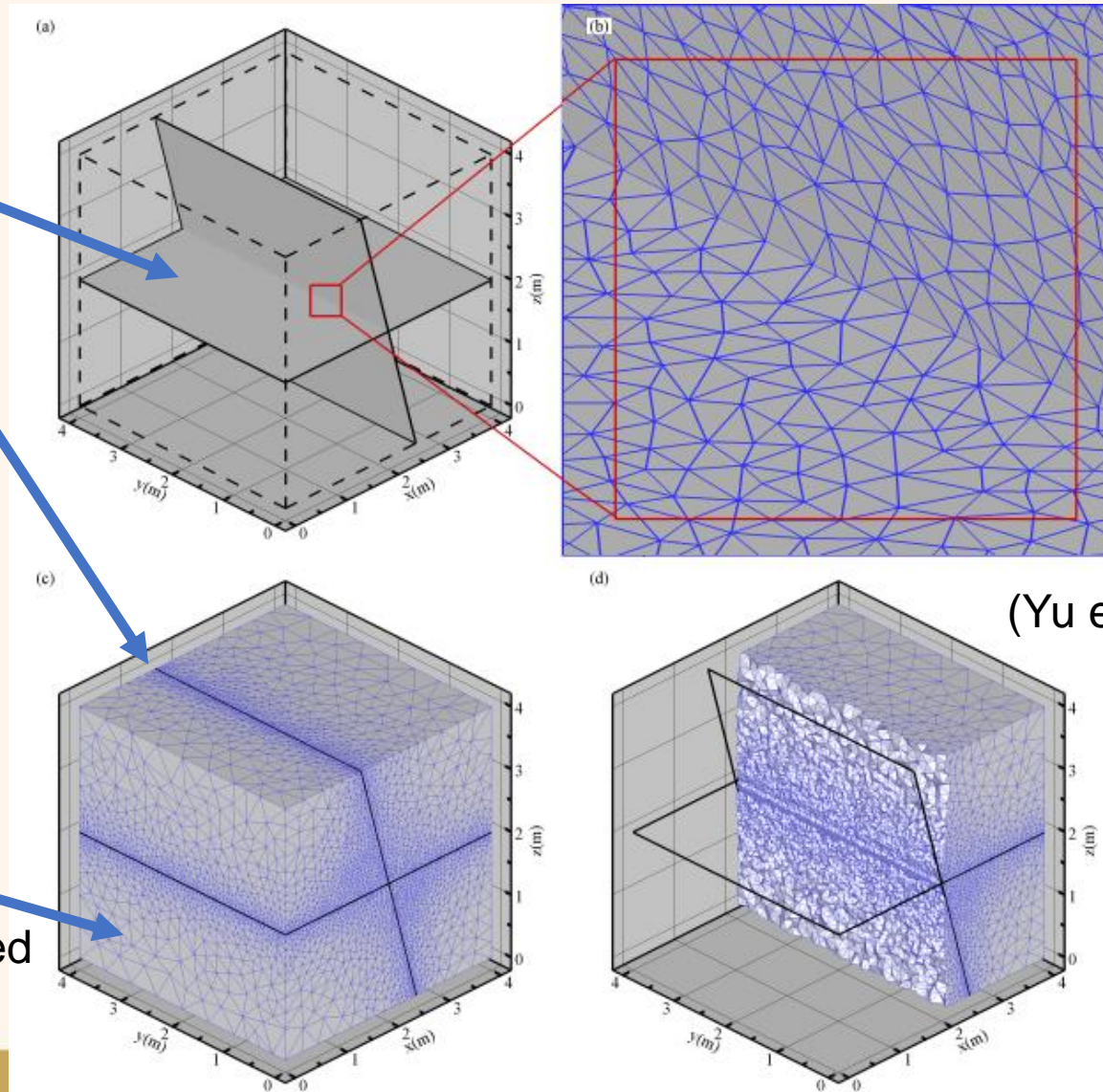
Two fractures with one collinear line

Fractures: triangular elements with arbitrary fracture apertures

$$\nabla \cdot [K(\mathbf{x})b(\mathbf{x})(\nabla h(\mathbf{x}))] + Q(\mathbf{x}) = 0$$

Matrix: Tetrahedral elements with physical flow (or transport) properties

Fractures and the 2D and 3D meshes for the proposed hybrid model.



(Yu et al., 2021)

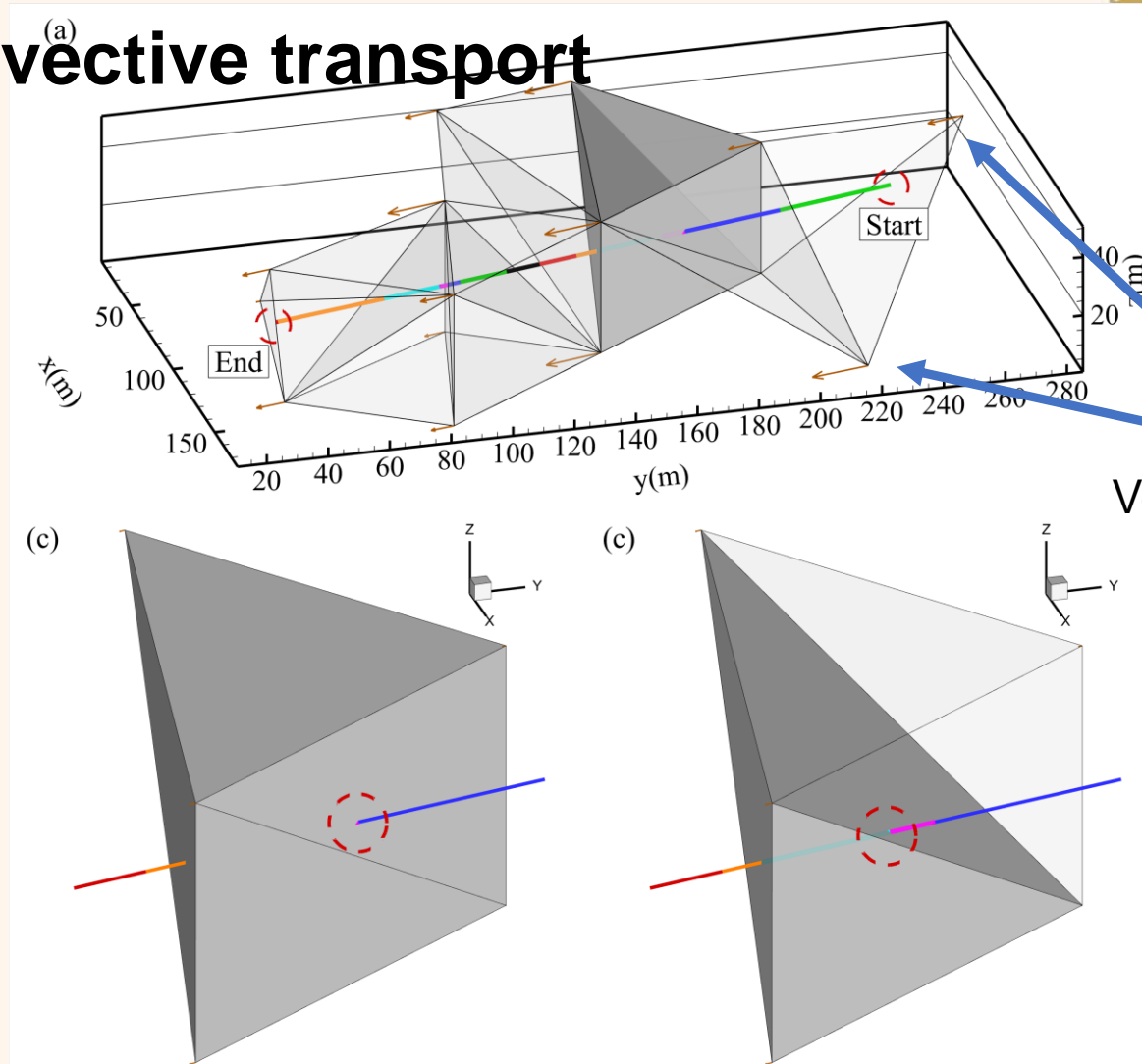
Numerical model – the concept

Particle tracking for advective transport

Ray-Plane test:
determine element faces &
intersection points.

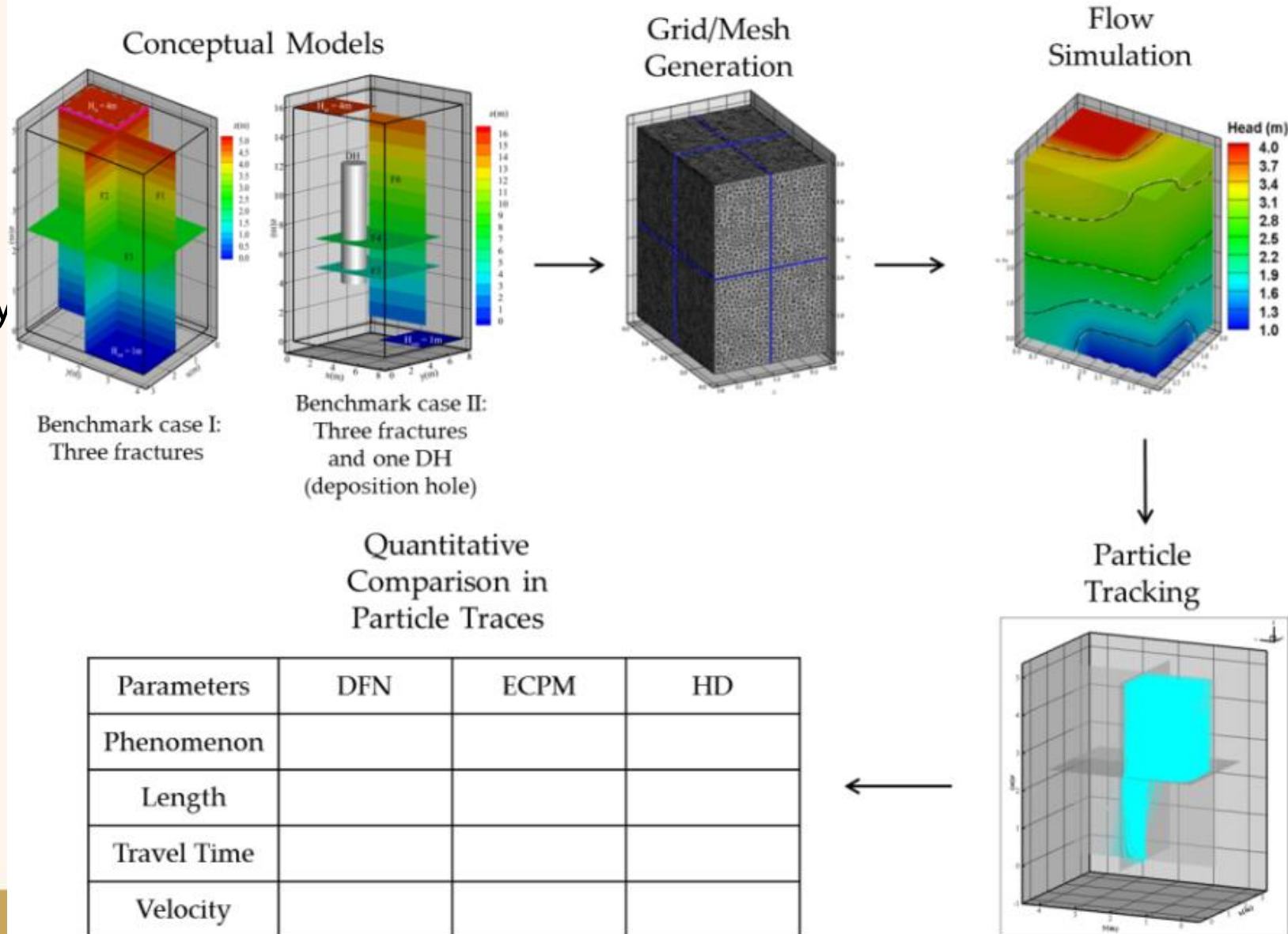
1. Point 3D velocities are calculated based on the velocities at nodes of the element face. (interpolation)
2. Traveling path follows the trajectory of the velocity vectors at the point on the element face.

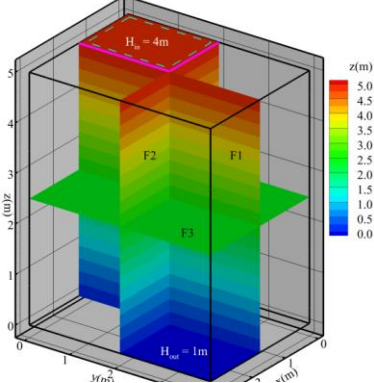
$$\frac{dx}{dt} = u(x,t)$$



Model tests

- The models
 - DFN → FracMan
 - ECPM → DarcyTools
 - Hybrid-domain HD (this study)
- Workflow
 - Mesh generation
 - Flow simulations
 - Particle tracking
- Two test cases
 - 3 intersected fractures
 - Fractures & deposition hole (DH)

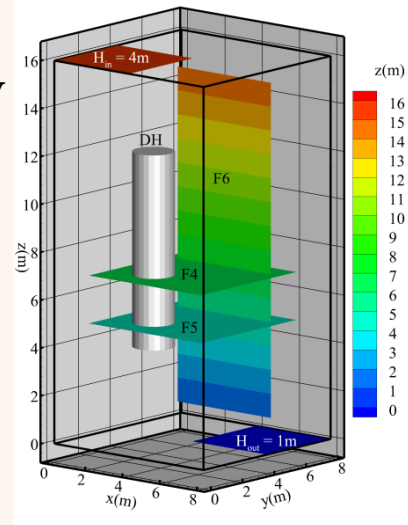




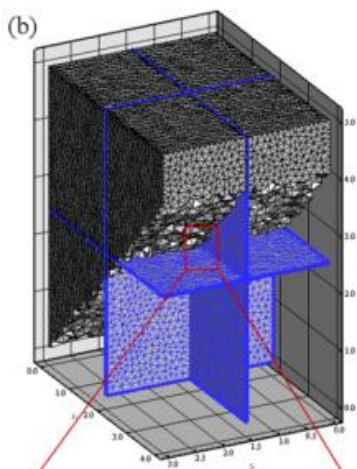
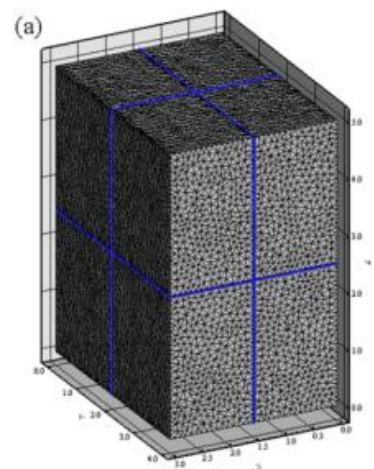
HD: 2D triangular and 3D tetrahedron elements are 9,147 and 290,324, respectively

ECPM model: 131,072 cells with 32, 64, and 64 in x-, y-, and z-directions

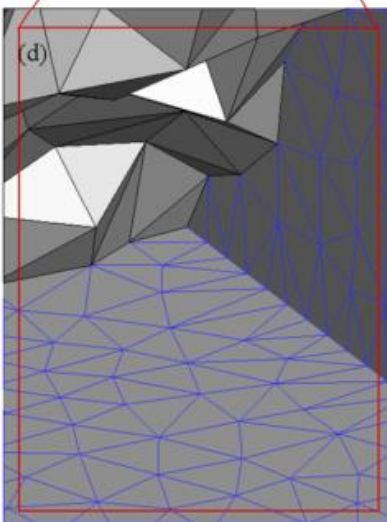
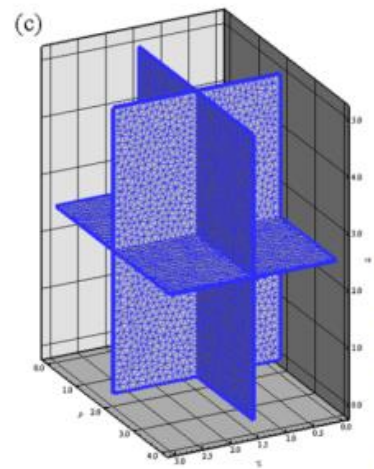
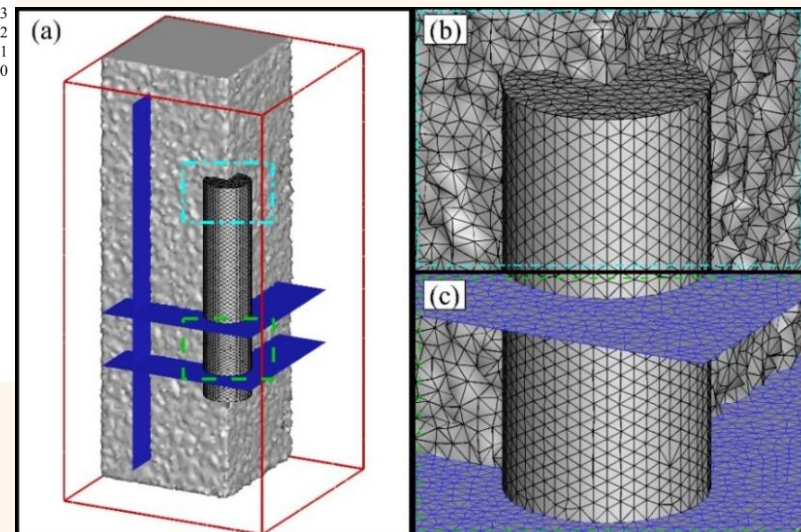
DFN: 12,624 elements



Not to scale



Fractures: FAB file from FracMan software

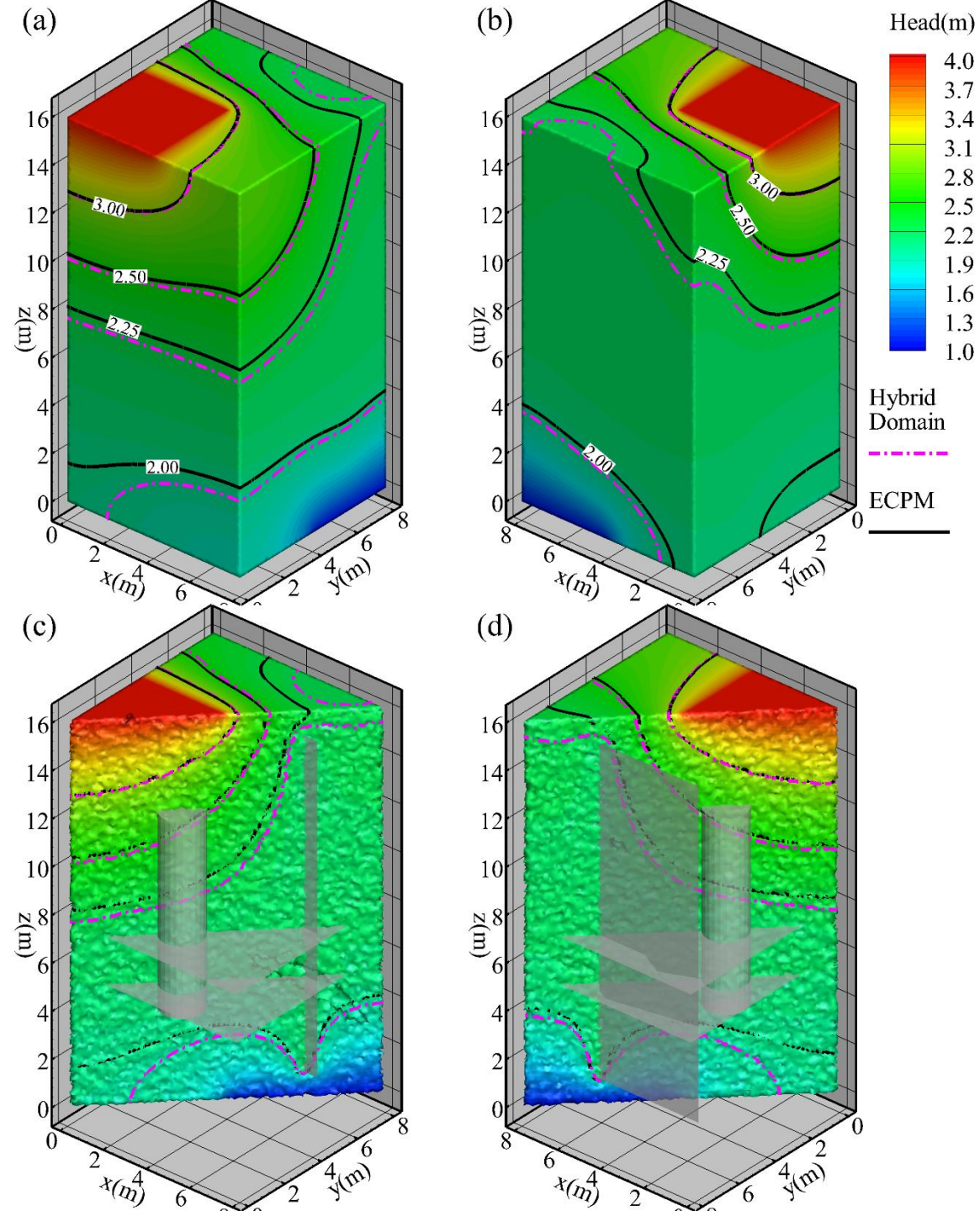
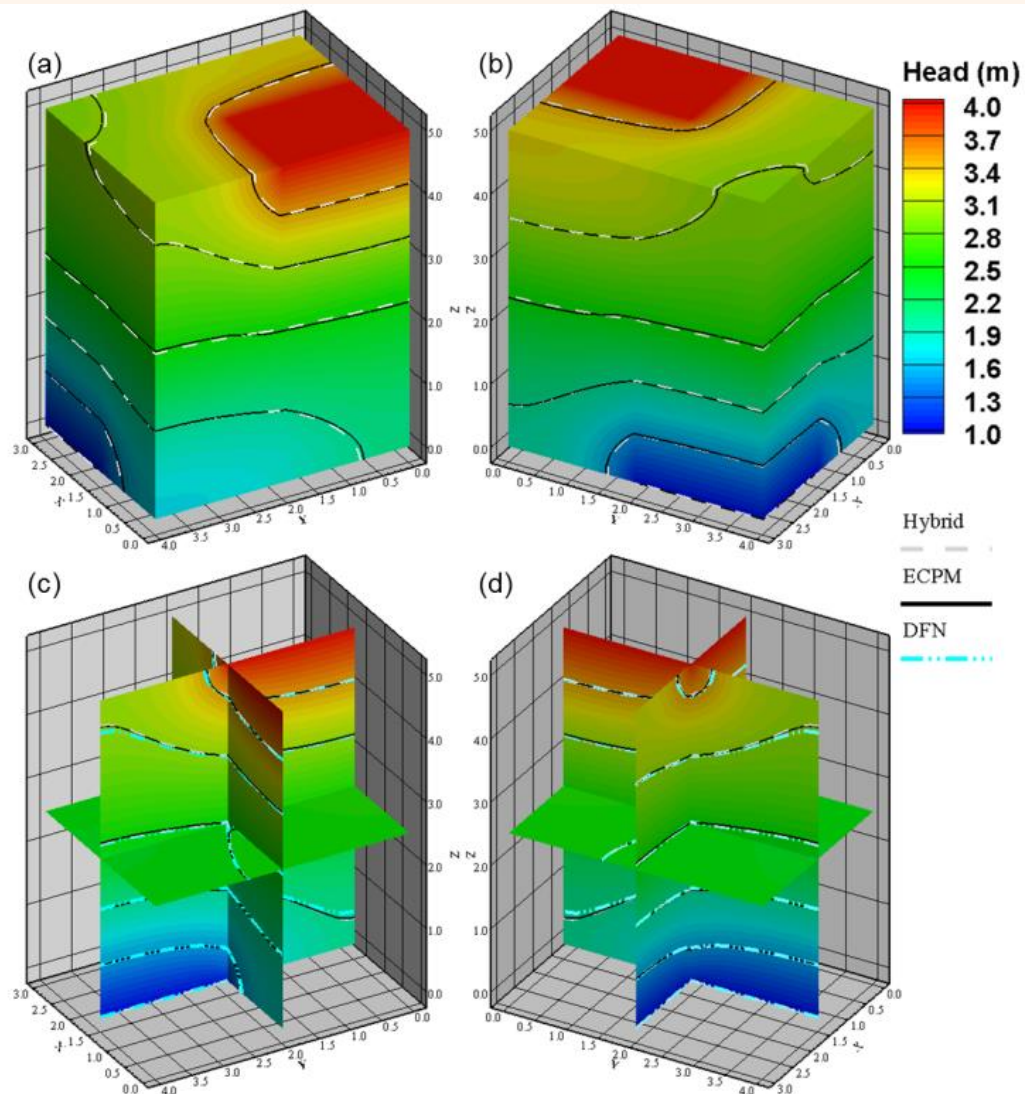


Parameters	Case I	Case II
Fracture transmissivity (m ² /s)	5.0×10^{-10}	5.0×10^{-7}
Matrix hydraulic conductivity (m/s)	1.0×10^{-10}	1.0×10^{-10}
Deposition hole hydraulic conductivity (m/s)	-	1.0×10^{-10}
Fracture aperture (m)	1.0×10^{-4}	1.0×10^{-1}
Fracture porosity (-)	4.0×10^{-1}	4.0×10^{-1}
Rock matrix porosity (-)	5.4×10^{-3}	5.4×10^{-3}
Convergence criteria (m)	1.0×10^{-8}	1.0×10^{-8}
Particle numbers (-)	1,000	1; 48 **

** There is a subcase with 48 particles for Case II.

Not to scale

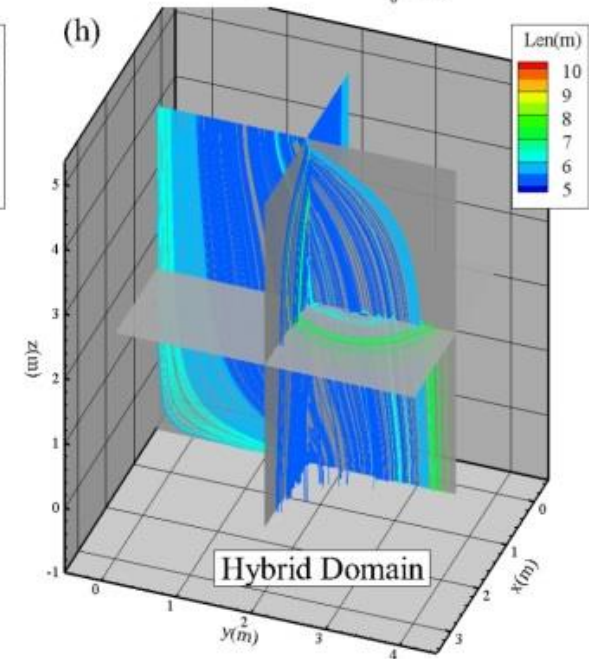
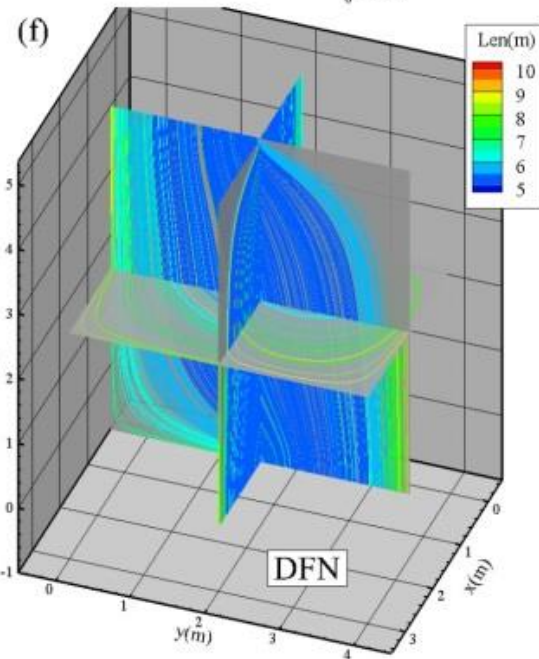
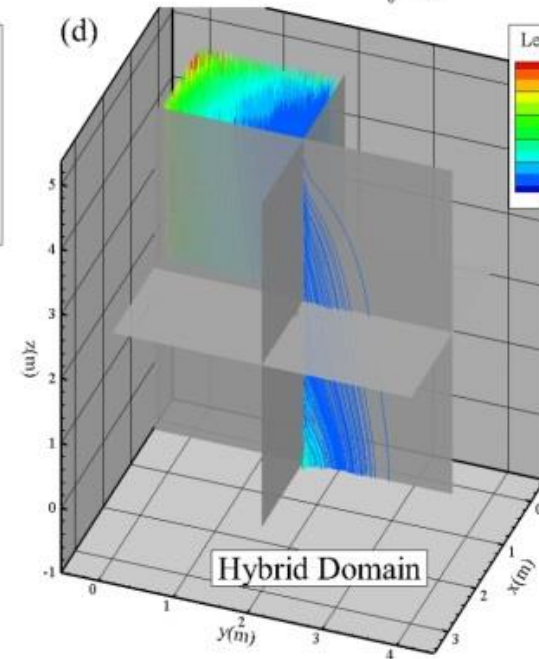
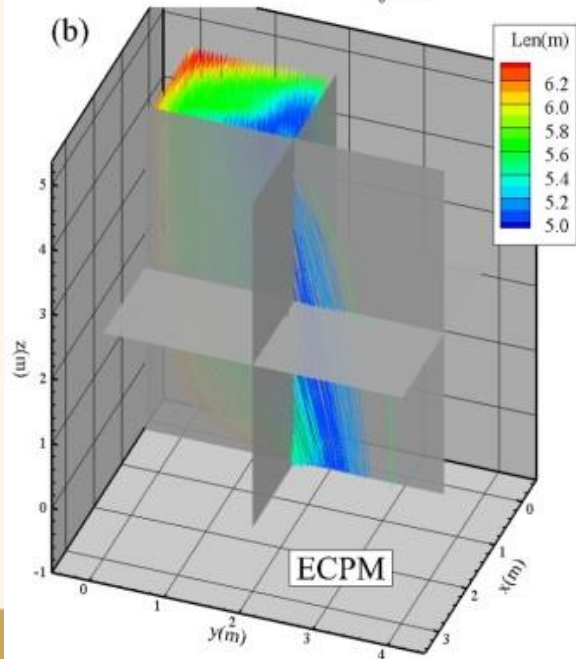
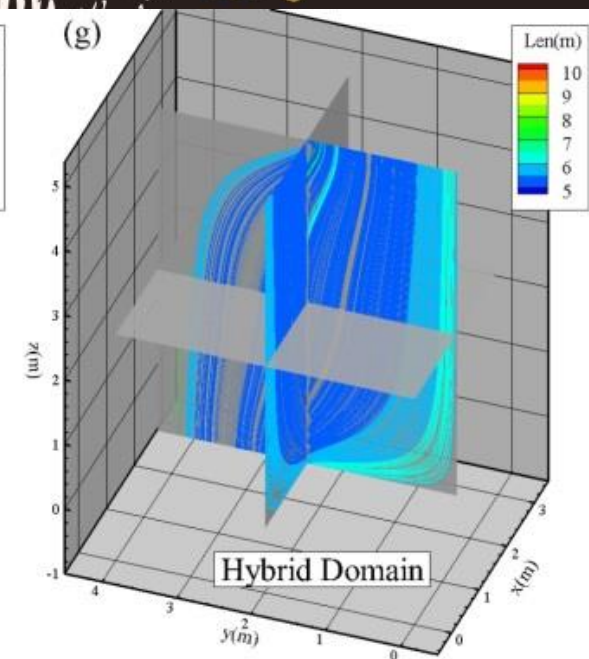
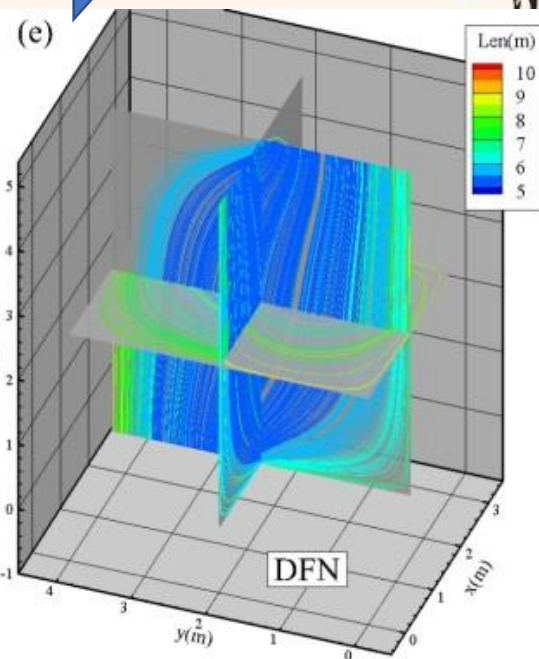
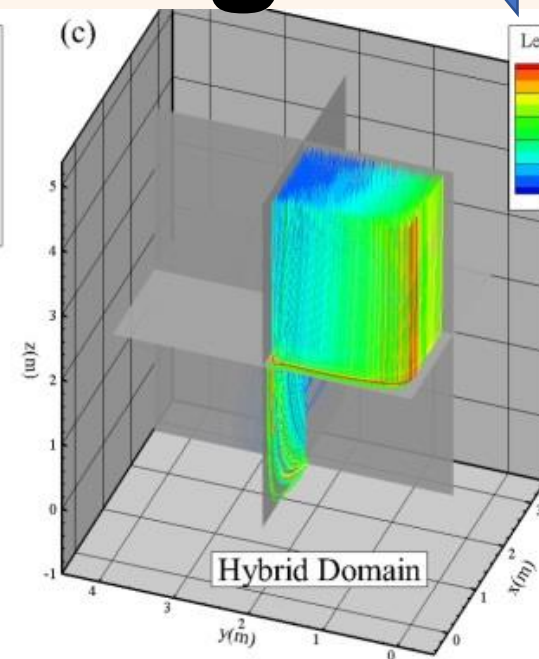
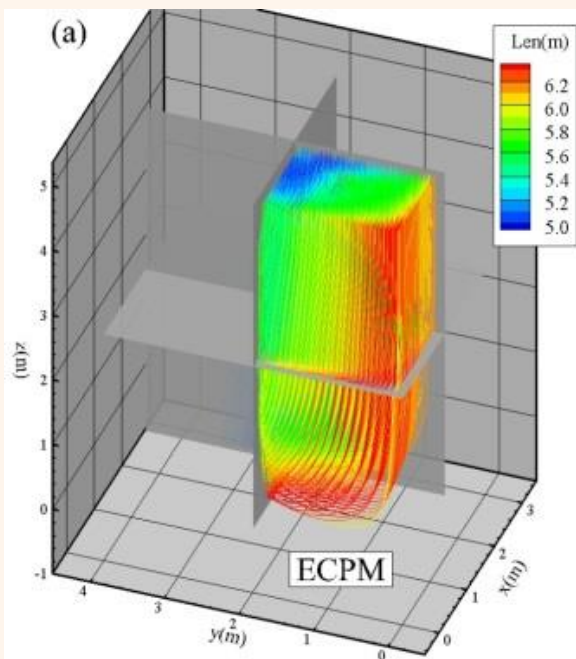
Flow simulations



Particle tracking



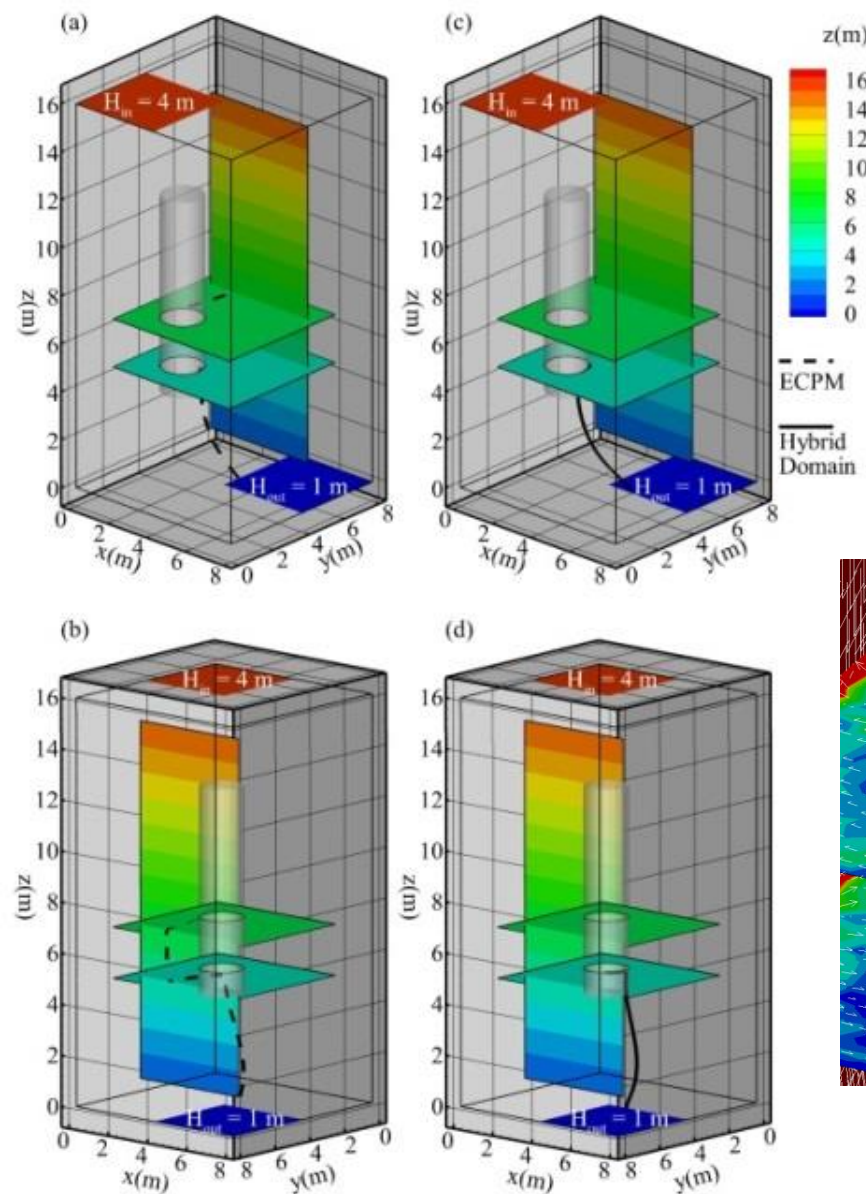
Fracture



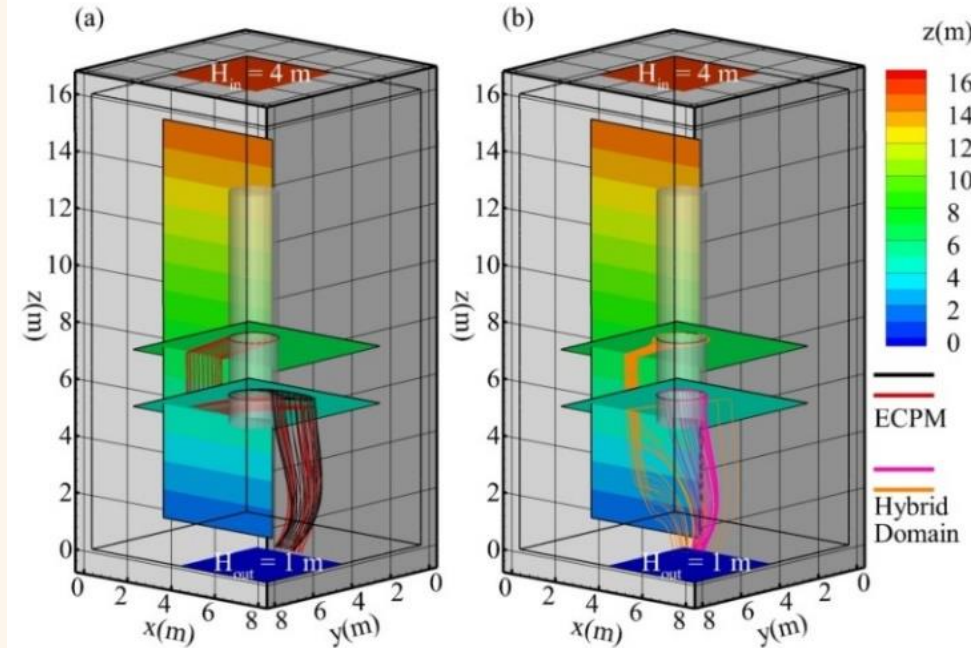
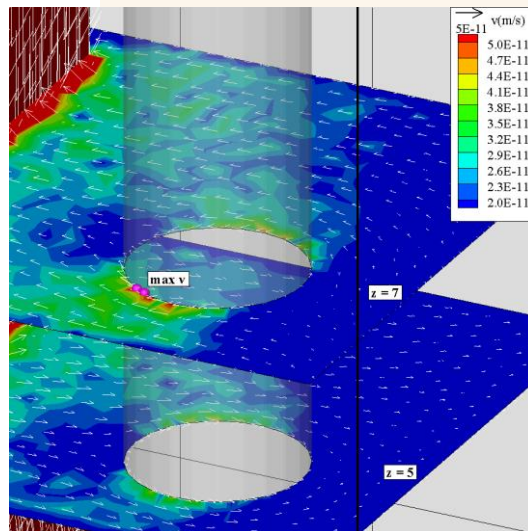
Statistics

Parameters		ECPM	HD (fractures and matrix)	DFN	HD (fractures only)
Trace length	Mean (m)	5.61	6.38	5.51	5.38
	STD (m)	0.35	1.01	0.63	0.37
	CV	0.062	0.158	0.114	0.069
	Min. (m)	5.07	5.12	5.11	5.10
	Max. (m)	6.39	10.48	9.04	7.77
Travel time	Mean (s)	4.0×10^8	2.1×10^8	3.2×10^6	3.9×10^6
	STD (s)	2.3×10^8	6.4×10^7	4.7×10^6	2.6×10^6
	CV	0.58	0.30	1.47	0.67
	Min. (s)	6.4×10^7	1.4×10^5	1.8×10^6	1.8×10^6
	Max. (s)	1.2×10^9	6.3×10^8	5.6×10^7	3.1×10^7
Velocity	Mean (m/s)	2.0×10^{-8}	1.5×10^{-7}	2.4×10^{-6}	6.5×10^{-6}
	STD (m/s)	1.4×10^{-8}	1.3×10^{-7}	6.2×10^{-7}	6.3×10^{-7}
	CV	0.70	0.87	0.26	0.10
	Min. (m/s)	5.1×10^{-9}	8.8×10^{-9}	2.0×10^{-7}	2.0×10^{-7}
	Max. (m/s)	8.0×10^{-7}	3.6×10^{-5}	2.8×10^{-6}	2.9×10^{-6}

ECPM & HD



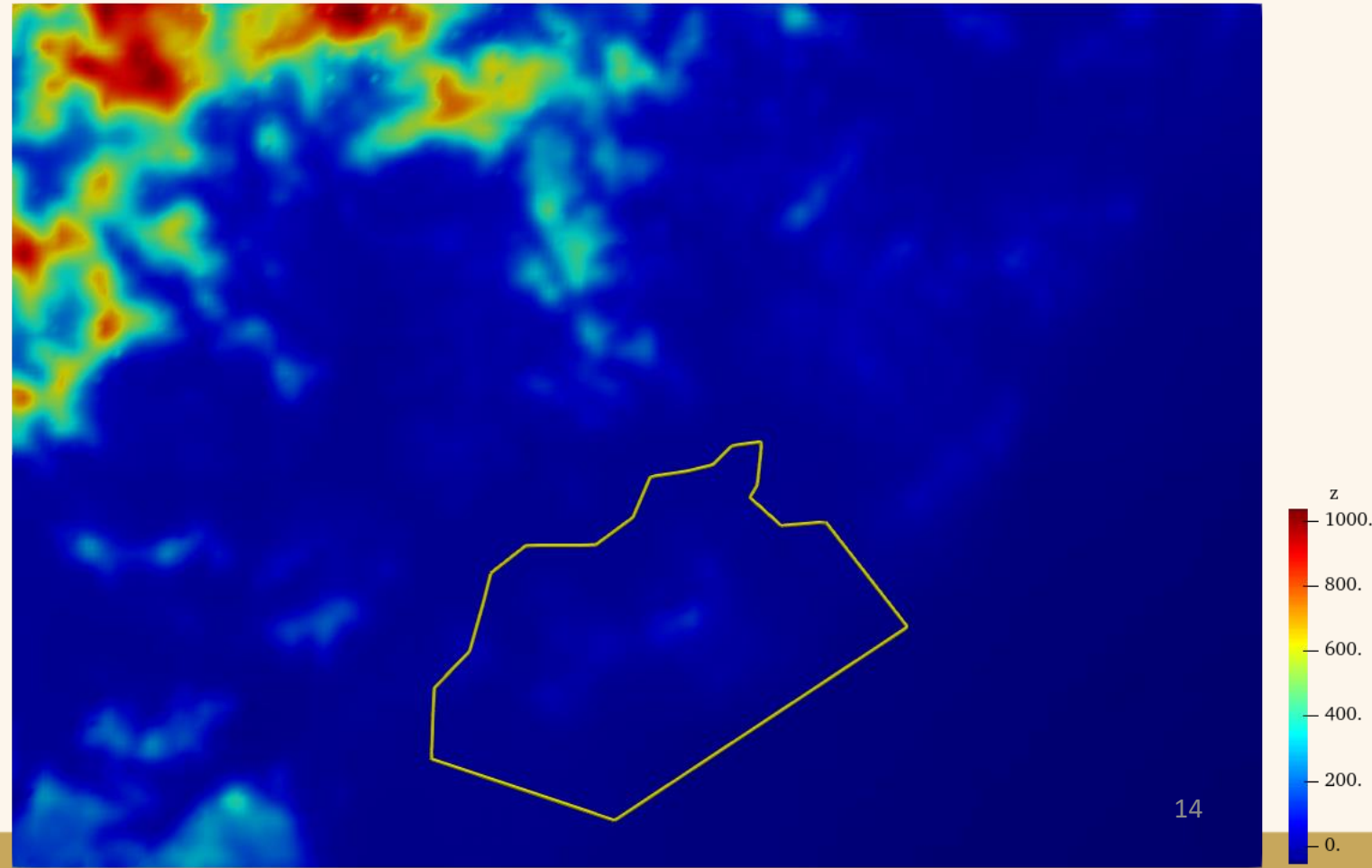
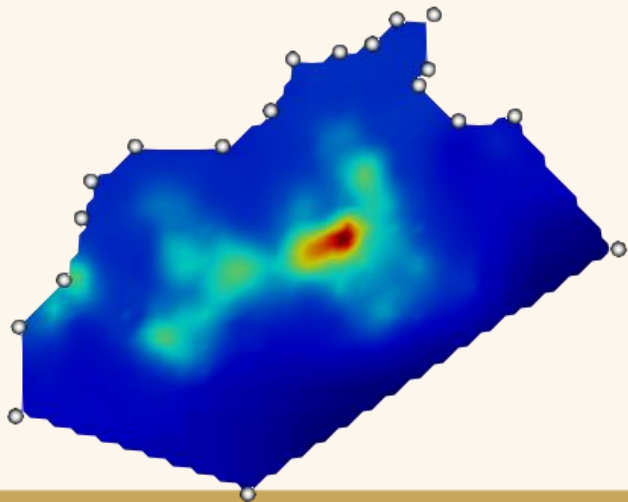
A particle released at the highest velocity location



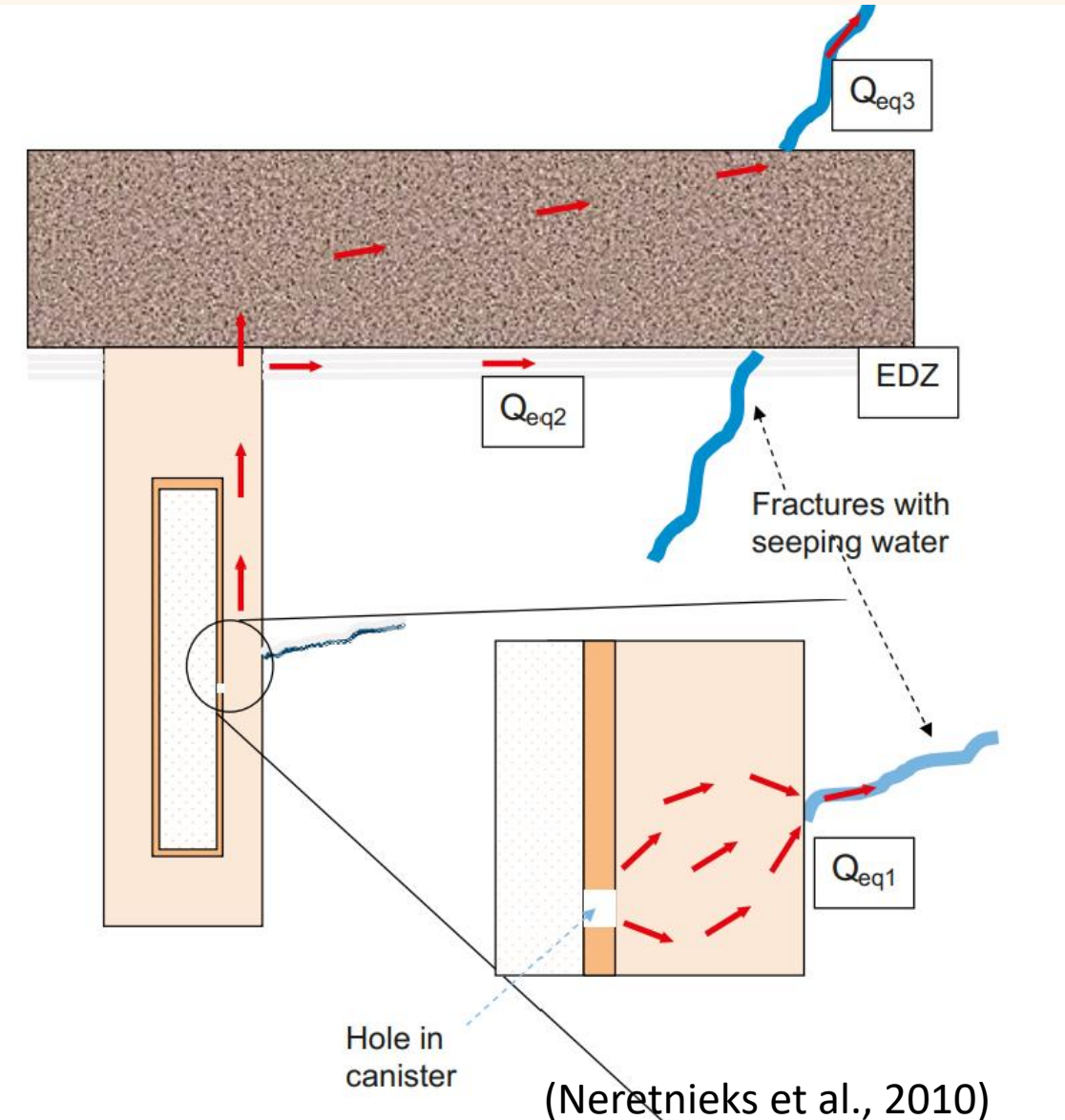
Parameters	ECPM model	HD model	
Trace length	Mean (m)	10.69	9.07
	STD (m)	3.16	2.74
	CV	0.296	0.302
	Min. (m)	7.25	5.85
	Max. (m)	15.70	15.10
Travel time	Mean (s)	9.70×10^9	4.25×10^9
	STD (s)	2.40×10^9	1.05×10^9
	CV	0.247	0.247
	Min. (s)	6.50×10^9	2.69×10^9
	Max. (s)	1.55×10^{10}	7.10×10^9
Velocity	Mean (m/s)	1.09×10^{-9}	2.18×10^{-9}
	STD (m/s)	1.56×10^{-10}	1.10×10^{-9}
	CV	0.143	0.505
	Min. (s)	8.31×10^{-10}	1.15×10^{-9}
	Max. (s)	1.37×10^{-9}	4.33×10^{-9}

Implementation:

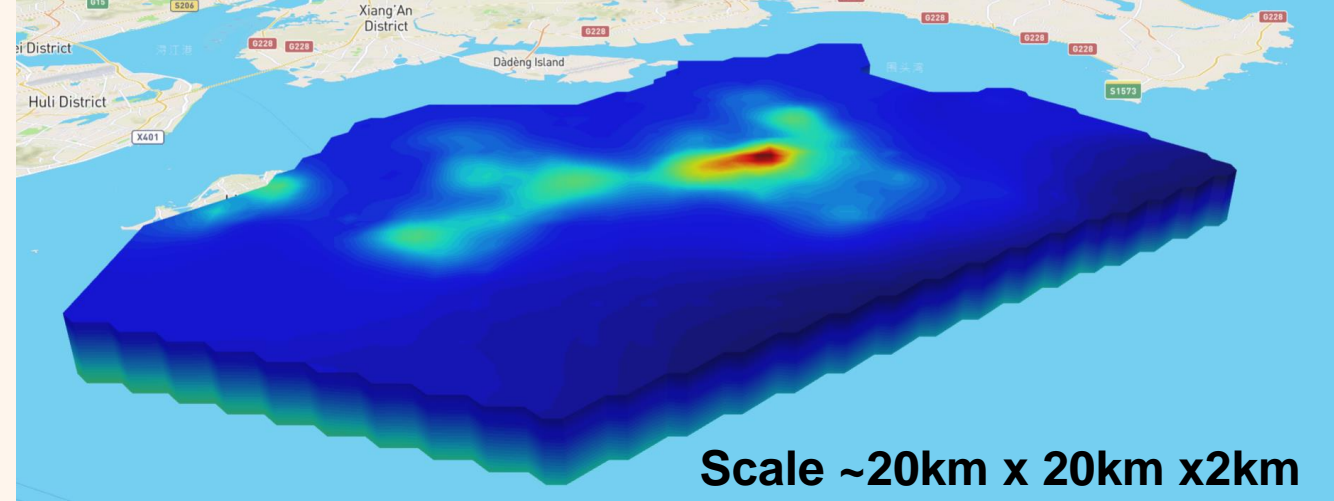
A case with practical scale and complexity



Objectives

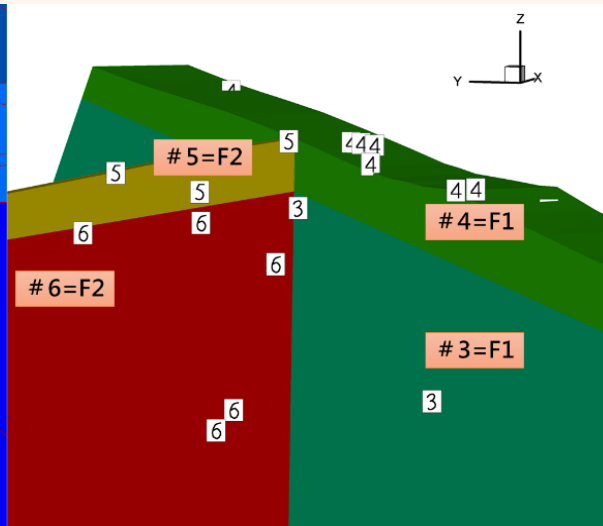
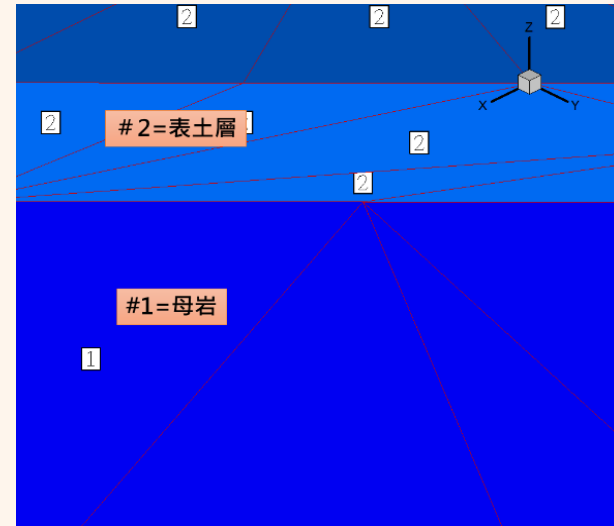


- Implementation of HD model for practical scale & complexity
- Conduct flow and advective transport in fractured formation (FAB)
- Search three main pathways, Q_1 , Q_2 , & Q_3
- Consider layout, main tunnel(MT), deposition tunnel(DT), deposition holes(DH), and excavation damage zone(EDZ) STL(**S**Tereo**L**ithography)
- Evaluate transport properties



Section07: DFN Recipe for R# (F# and D# are assumed to be deterministic structures and treated as porous media)

	FDMA	FDMB-
Fracture Domain-	Elevation (depth below surface, m) < 70 m-	Elevation (depth below surface, m) > 70 m-
Fracture clusters- (Pole_Trend, Pole_Plunge)	Cluster 1 = (198, 18), Fish distribution ($\theta, \kappa = 18$), $P_{32,rel} = 26\%$ -	Cluster 1 = (65, 17), Fish distribution ($\theta, \kappa = 20$), $P_{32,rel} = 15\%$ -
	Cluster 2 = (155, 4), Fish distribution ($\theta, \kappa = 15$), $P_{32,rel} = 24\%$ -	Cluster 2 = (344, 38), Fish distribution ($\theta, \kappa = 18$), $P_{32,rel} = 24\%$ -
	Cluster 3 = (264, 23), Fish distribution ($\theta, \kappa = 16$), $P_{32,rel} = 18\%$ -	Cluster 3 = (281, 29), Fish distribution ($\theta, \kappa = 16$), $P_{32,rel} = 30\%$ -
	Cluster 4 = (98, 81), Fish distribution ($\theta, \kappa = 11$), $P_{32,rel} = 32\%$ -	Cluster 4 = (174, 22), Fish distribution ($\theta, \kappa = 17$), $P_{32,rel} = 10\%$ -
	Cluster 5 = (175, 75), Fish distribution ($\theta, \kappa = 19$), $P_{32,rel} = 21\%$ -	
	Fisher distribution $f(\theta, \kappa) = \frac{\kappa \sin \theta e^{\kappa \cos \theta}}{\pi^2 (1 + \kappa^2)}$; - θ = the angular displacement from the mean pole vector- κ = a concentration parameter of Fisher distribution-	
Fracture intensity-	$P_{32} = 2.4$ -	$P_{32} = 0.3$ -
	P_{32} = Area of fractures per unit volume of rock mass (volumetric intensity, m^{-1})-	
Fracture size-	Power law : $k_r = 2.6, r_0 = 0.1 m, r_{min} = 4.5 m, r_{max} = 564 m$ -	Power law : $k_r = 2.6, r_0 = 0.1 m, r_{min} = 4.5 m, r_{max} = 564 m$ -
	$P(R \geq r) = \left(\frac{r_0}{r}\right)^{k_r}, P_{32}(r_{min}, r_{max}) = \left[\frac{r_{min}^{k_r-2} - r_{max}^{k_r-2}}{r_0^{k_r-2}}\right] P_{32}(r_0, \infty)$ -	
	R is the fracture radius- r_0 is the minimum radius value- r is any fracture radius between r_0 and ∞ -	
	k_r is the exponent of fractal dimension, or the "fracture radius scaling exponent" (La Pointe, 2002, p381)- $P(R \geq r)$ is the probability that a circular-shape fracture with a radius greater than or equal to r - $P_{32}(r_{min}, r_{max})$ is the volumetric fracture intensity corrected with determined fracture radius between r_{min} and r_{max} -	
Fracture location-	Stationary random (Poisson) process-	Stationary random (Poisson) process-
Fracture Transmissivity ($T, m^2/s$)	$T = a_1 \times (r)^b = a_2 \times (L)^b$ for FracMan/MAFIC; $T = a_3 \times (L_f/100)^b$ for DarcyTools- $\pi r^2 = L^2 = (L_f/100)^2$; $a_2 = a_1 \times (\pi)^{-0.5b}$; $a_3 = a_2 \times (100)^b = a_1 \times (\pi)^{-0.5b} \times (100)^b$ -	
	r : radius (m) of a disk fracture; L : equivalent size (m) of a square fracture, m; L_f : physical length (m) of an intersecting fracture in orthogonal direction-	
Fracture Aperture (e, m)	$e = 0.5\sqrt{T}$ -	$e = 0.5\sqrt{T}$ -
Source-	SNFD-SKBI-PL2015-1023; Vidstrand et al., 2010, p107-	SNFD-SKBI-PL2015-1023; Vidstrand et al., 2010, p106-

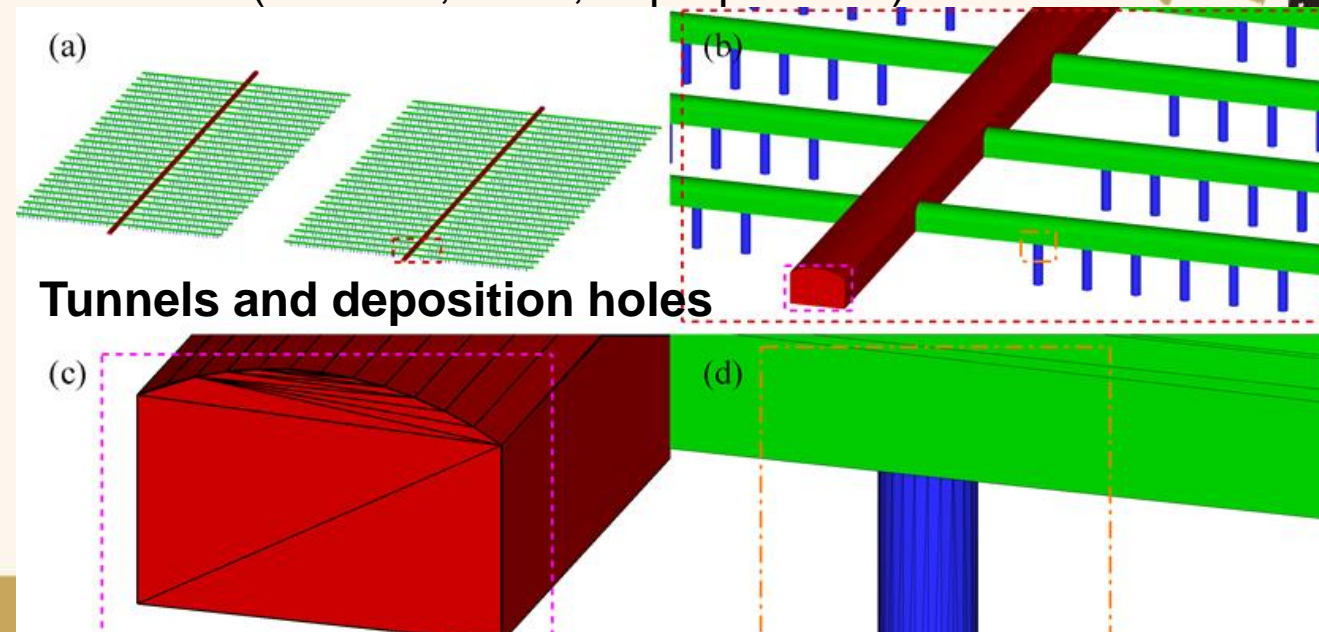


**Main rock formations
70m above and below**

Faults

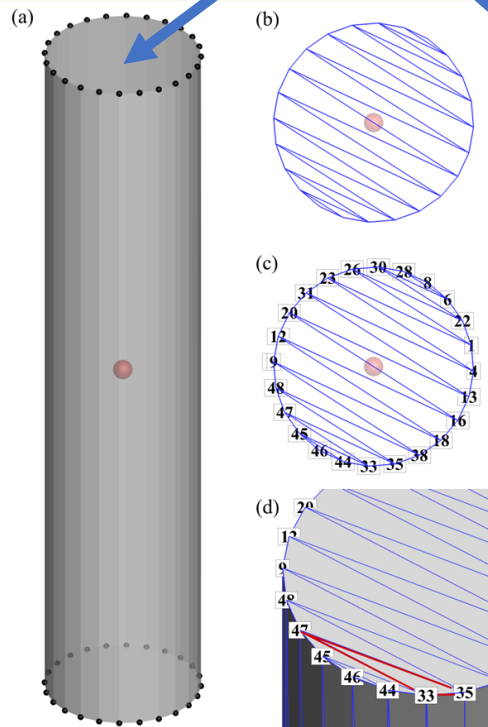
DFN recipe: 70m above and below

(Yu et al., 2022, in preparation)

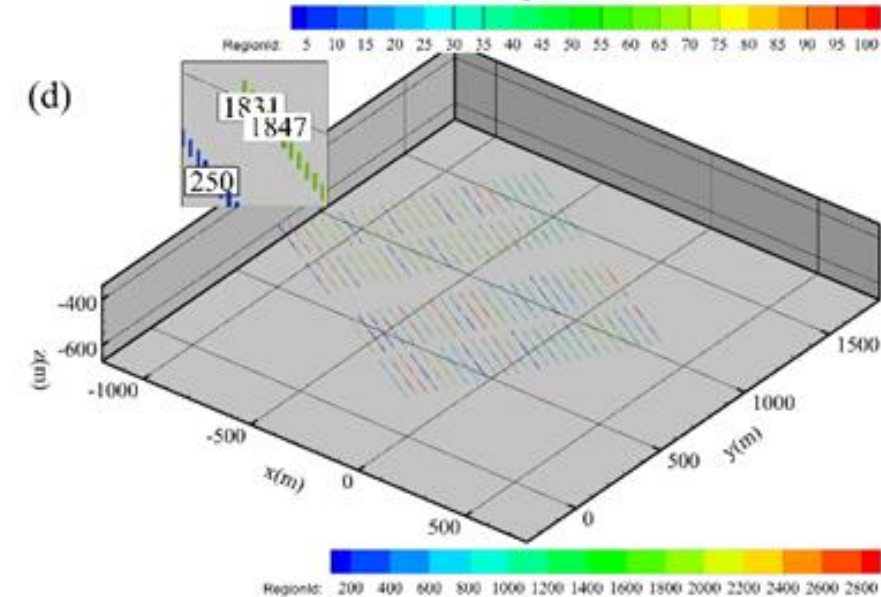
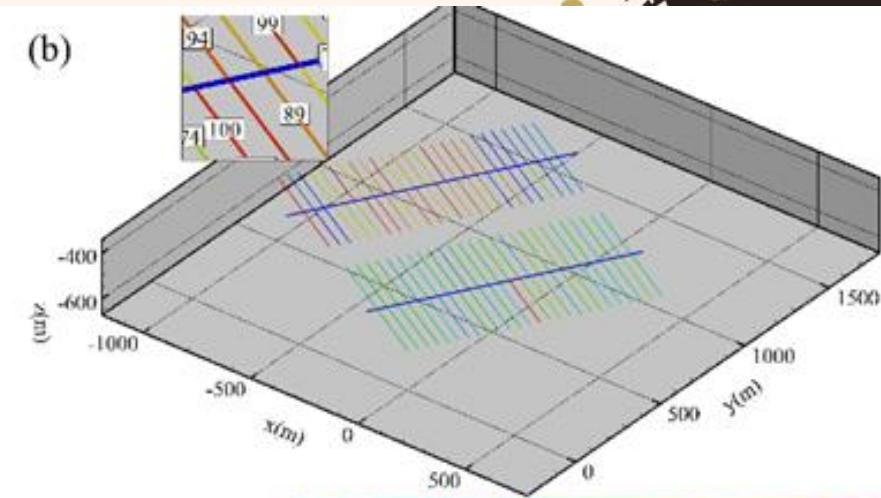
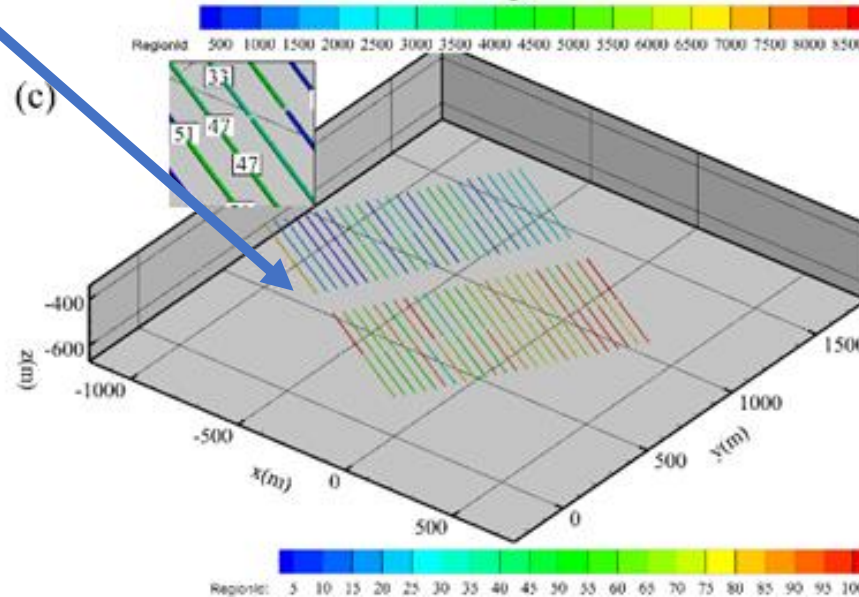
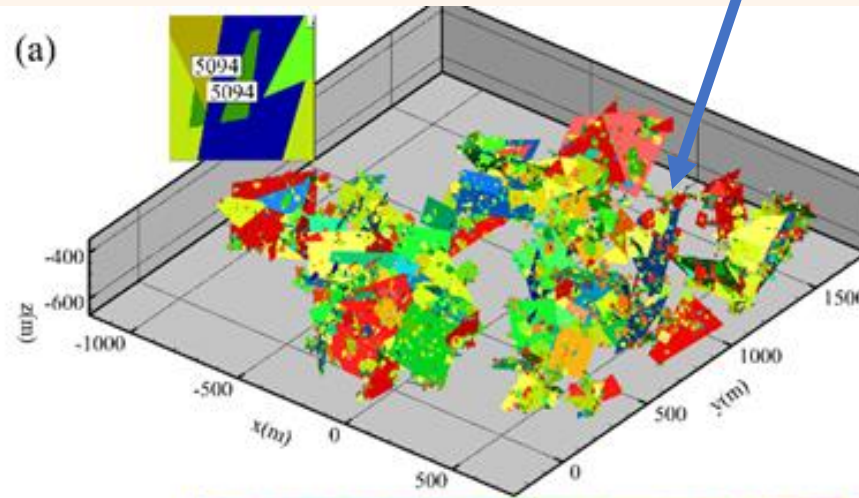


Tunnels and deposition holes

STL files for MT, DT, DH, and EDZ

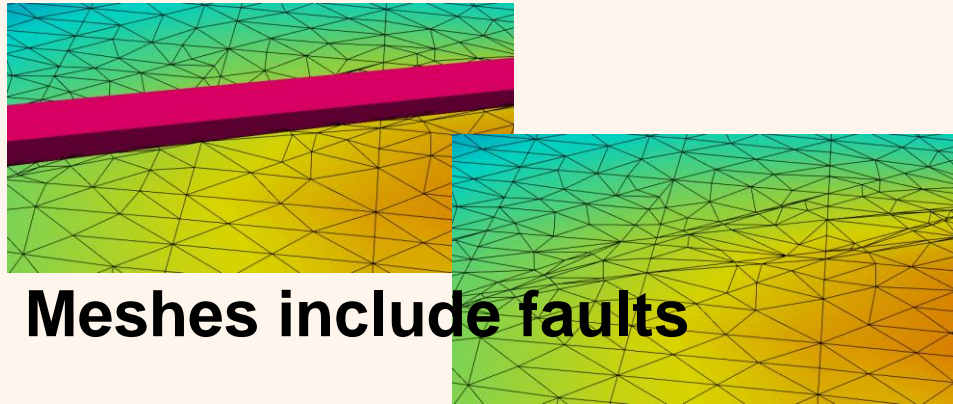


Read DFN FAB file from FracMan

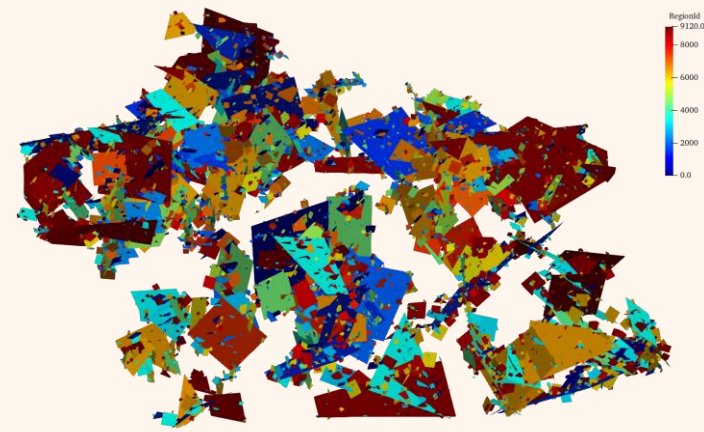
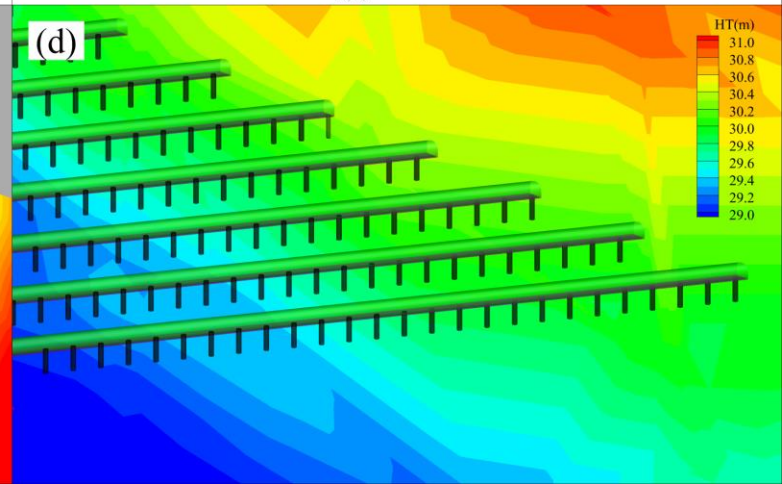
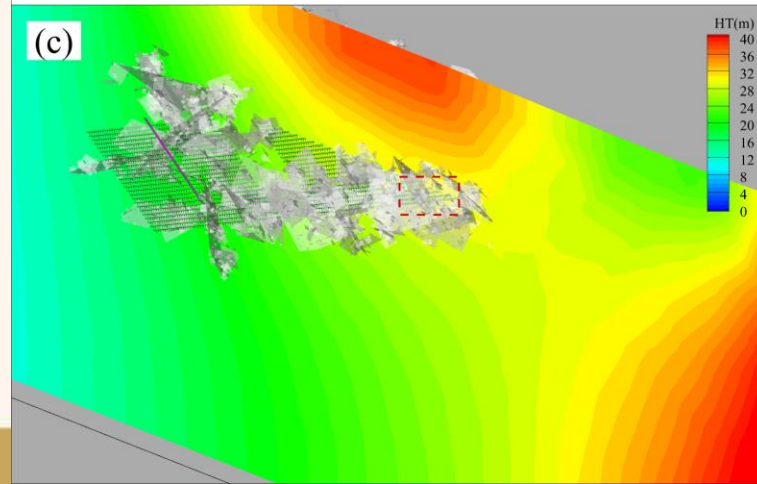
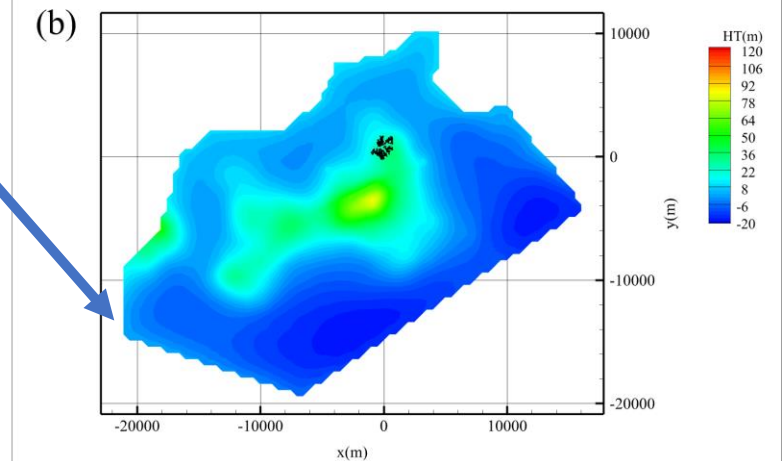
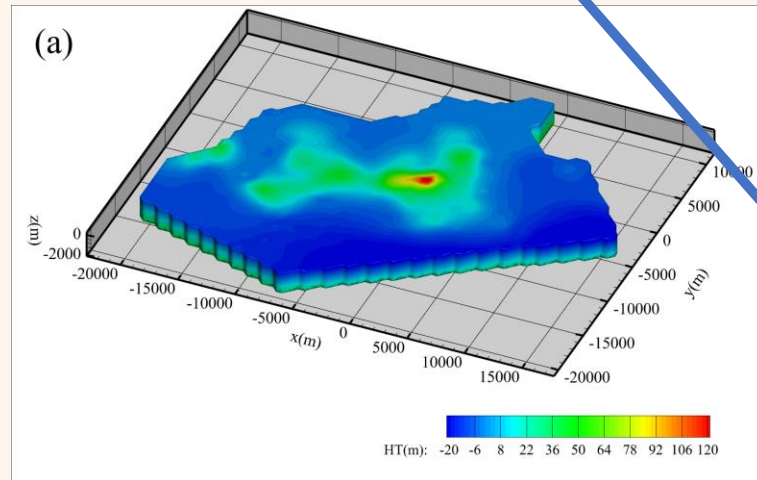


Flow simulation

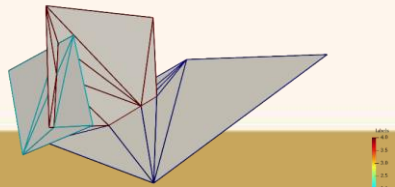
Specified head B.C. for steady state flow



Meshes include faults

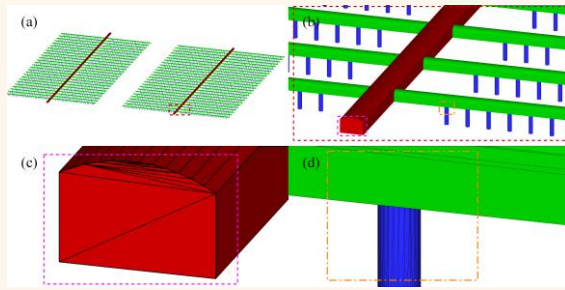


Fractures and the generation of mesh

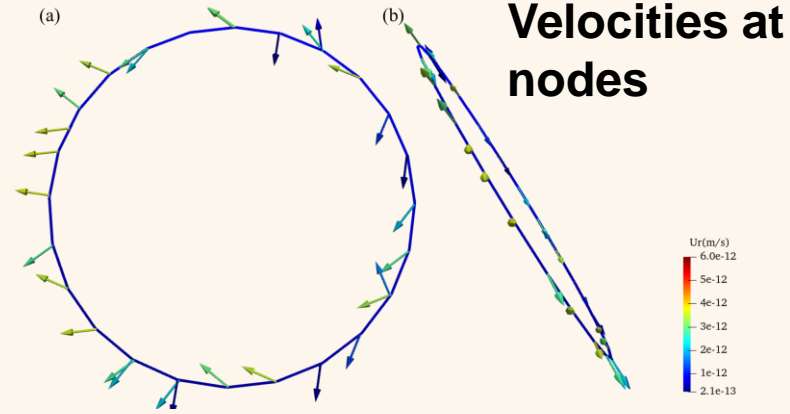
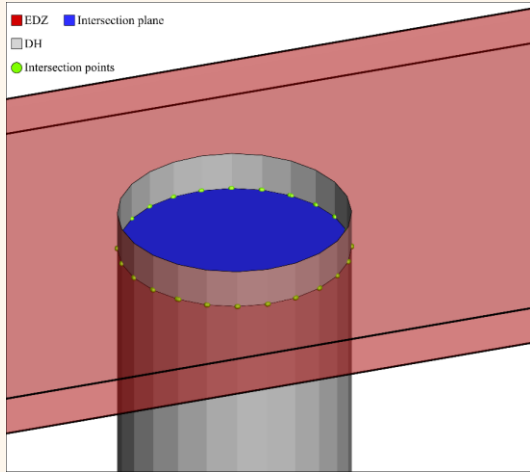
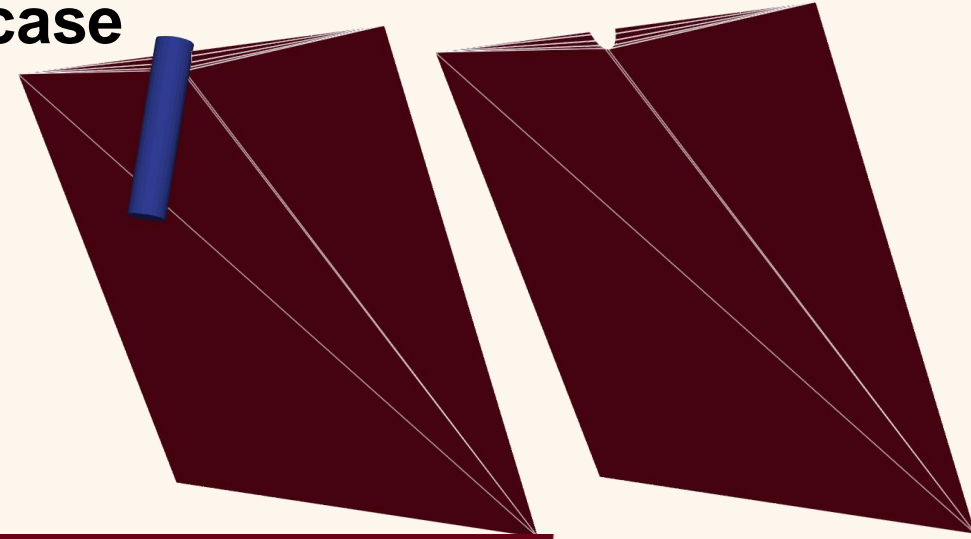


Intersections

Floating-point Arithmetic(Cherchi et al, 2020)

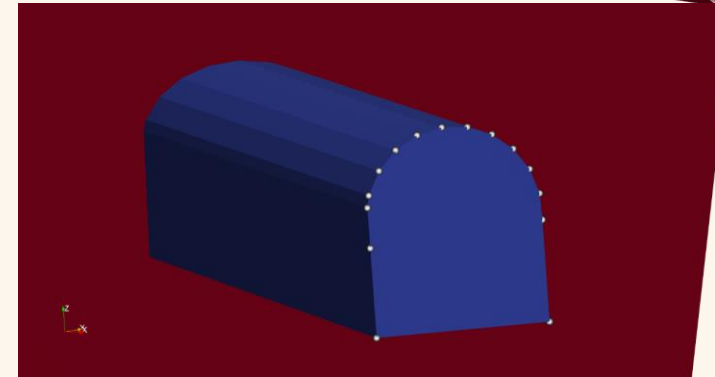


Q1 partially intersected case

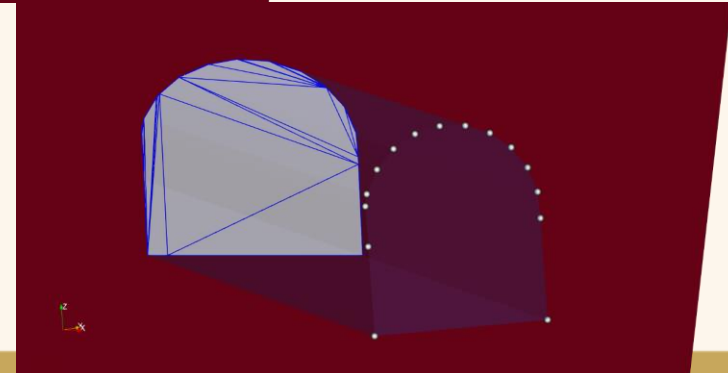


Q2 fully intersected case

Path	Type	Intersection	File name
Q1	Full	160	Q1Full.csv
Q1	Partial	34	Q1Part.csv
Q2	Full	2861	Q2Full.csv
Q2	Partial	0	Q2Part.csv
Q3	Full	109	Q3Full.csv
Q3	Partial	110	Q3Part.csv



Q3 fully intersected case



Particle tracking

Potential paths	Initial flux (m/s)	Location
Q1	6.746797×10^{-12}	224.01288, 567.0276, -500.0
Q2	6.746917×10^{-12}	223.14775, 567.361, -500.3
Q3	6.746797×10^{-12}	220.6712, 570.88324, -496.6415

Travel time t_r

$$Q1 = 1.30812 \times 10^{16} \text{ (s)}$$

$$Q2 = 1.30888 \times 10^{16} \text{ (s)}$$

$$Q3 = 1.77045 \times 10^{16} \text{ (s)}$$

Darcy velocity U_r

$$Q1 = 6.746797 \times 10^{-12} \text{ (m/s)}$$

$$Q2 = 6.746917 \times 10^{-12} \text{ (m/s)}$$

$$Q3 = 6.746797 \times 10^{-12} \text{ (m/s)}$$

Equivalent flux Q_{eq}

$$Q1 = 2.190107 \times 10^{-16} \text{ (m}^3\text{/s)}$$

$$Q2 = 1.025728 \times 10^{-11} \text{ (m}^3\text{/s)}$$

$$Q3 = 1.770446 \times 10^{-15} \text{ (m}^3\text{/s)}$$

Travel length L_r

$$Q1 = 8323.562 \text{ (m)}$$

$$Q2 = 8316.176 \text{ (m)}$$

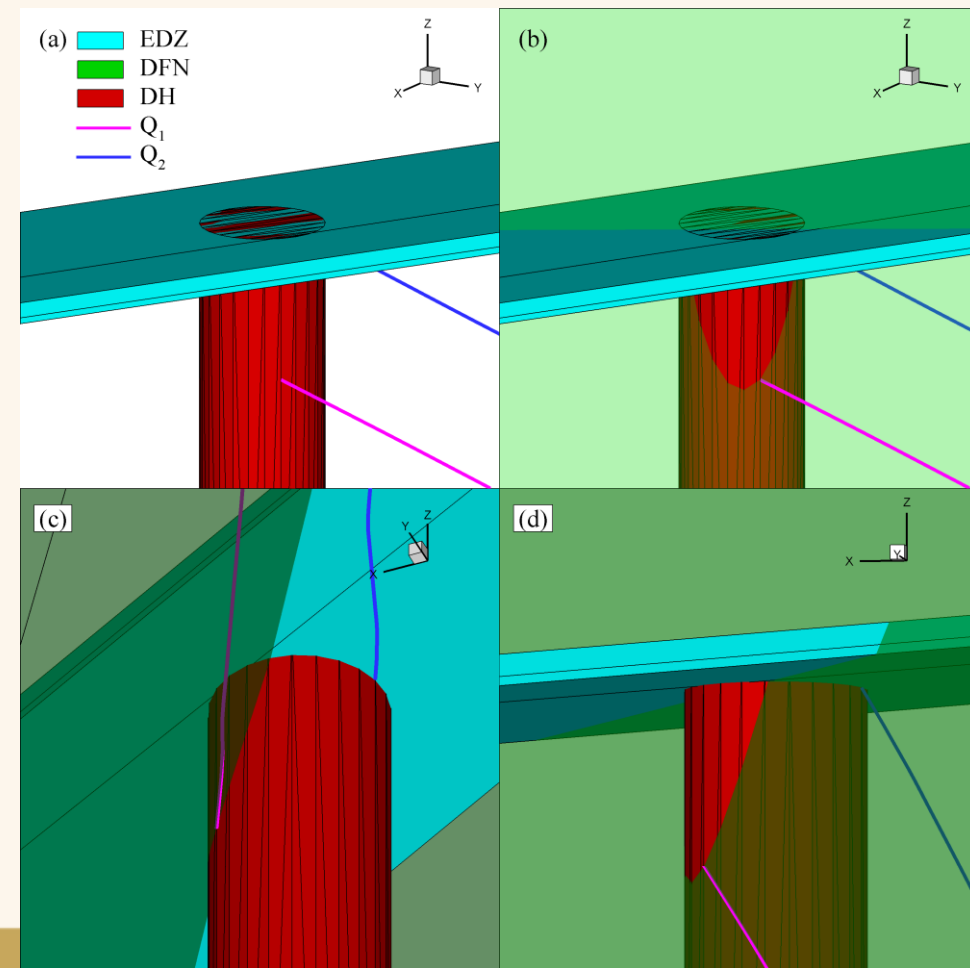
$$Q3 = 7664.157 \text{ (m)}$$

Transport resistance F_r

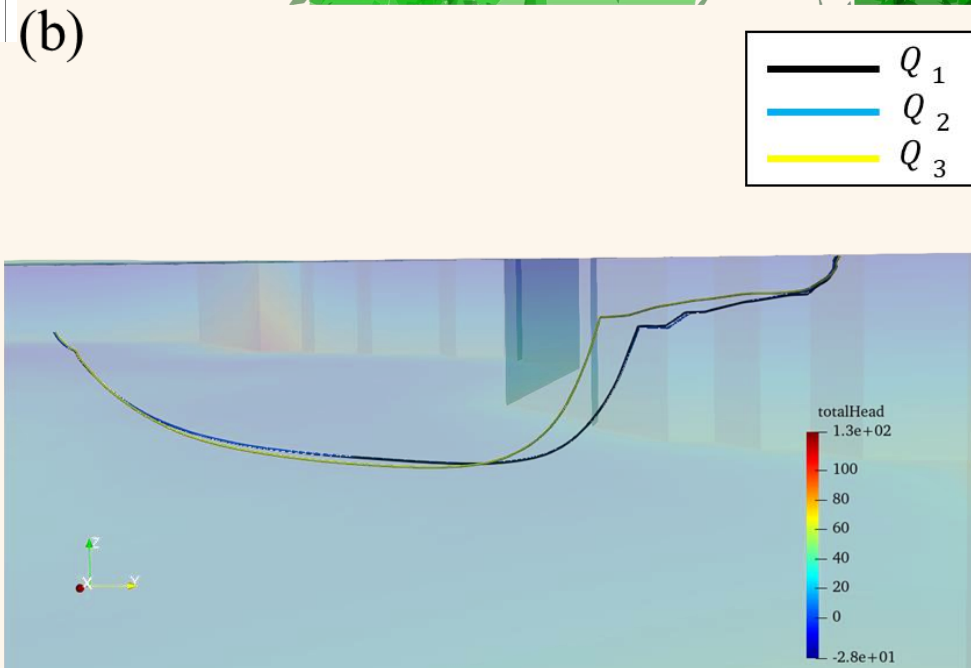
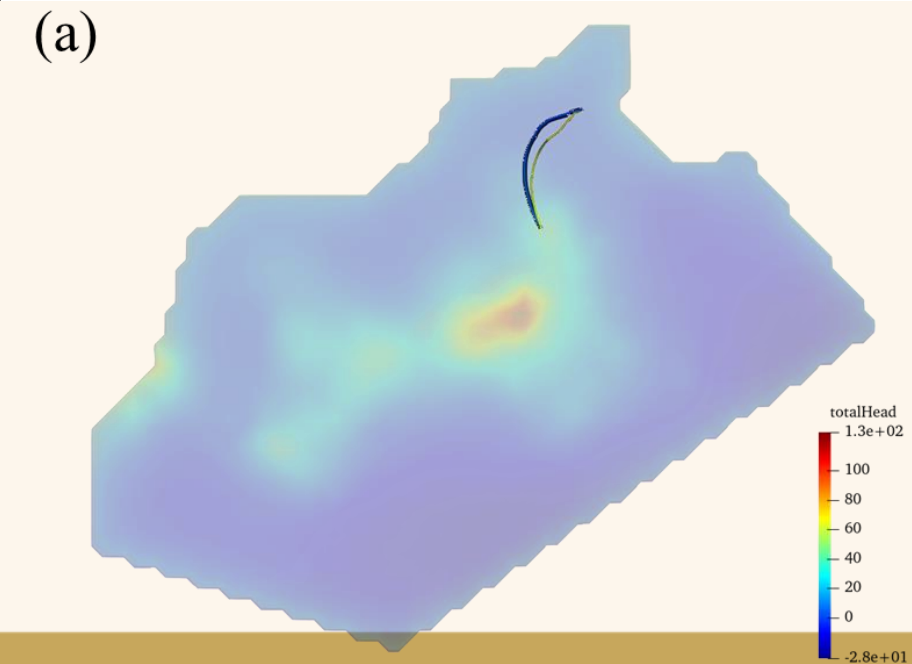
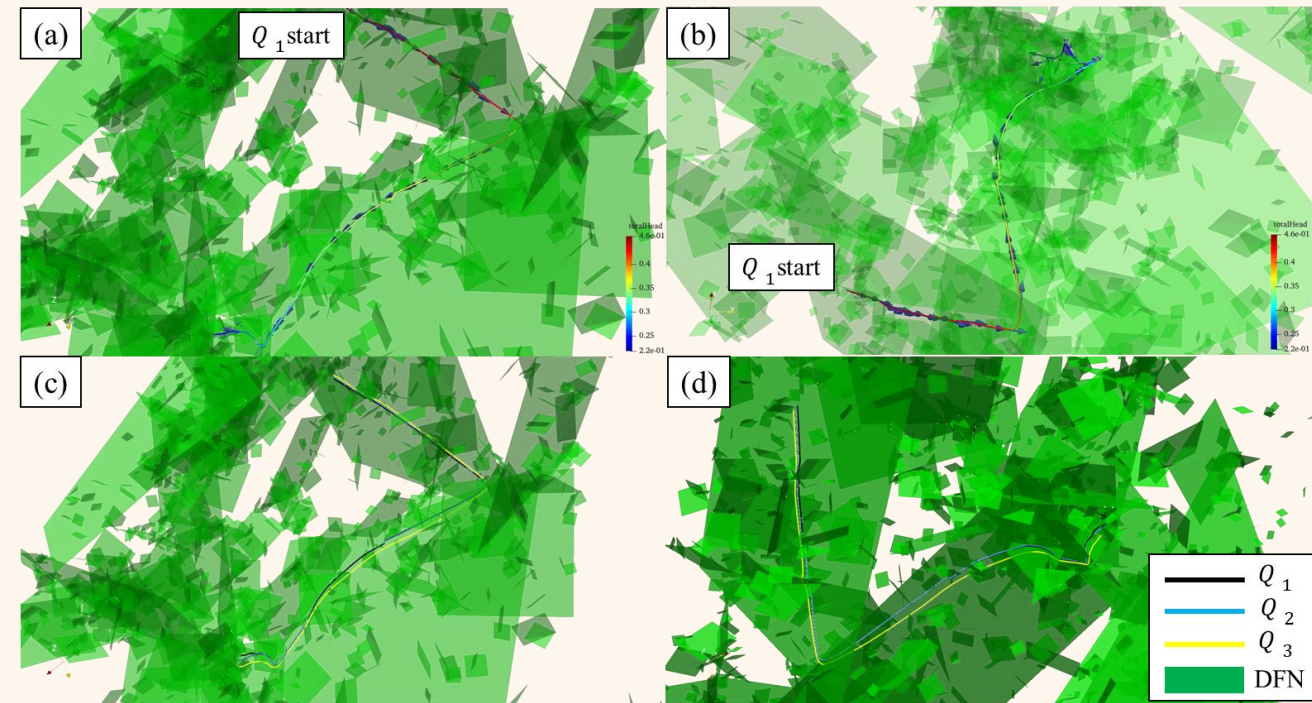
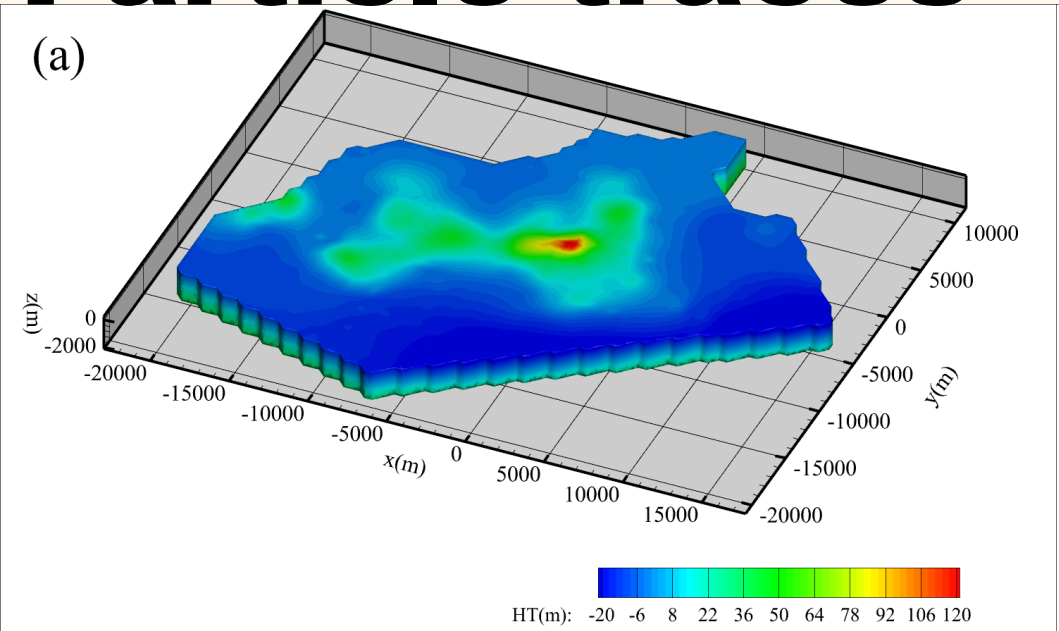
$$Q1 = 6.2745881 \times 10^{16}$$

$$Q2 = 6.2783641 \times 10^{16}$$

$$Q3 = 5.3679468 \times 10^{16}$$



Particle traces



Conclusion

- The study has developed the HD approach for the simulation of advective transport in fractured rocks.
- HD model is flexible in considering the concepts of DFN, ECPM, or both.
- A regional-scale case with objects of a disposal facility was employed to evaluate the developed model.
- Results show that the objects of a disposal facility and predefined DFN could be included in the HD model, and the intersections between disposal facility and fractures has been obtained successfully.



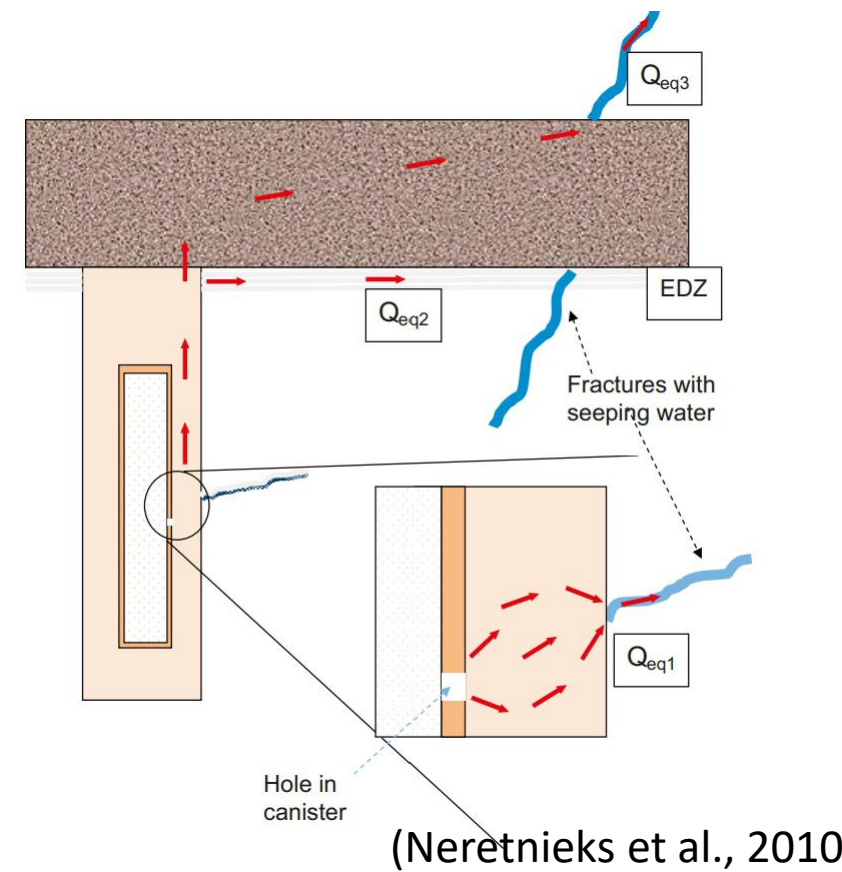
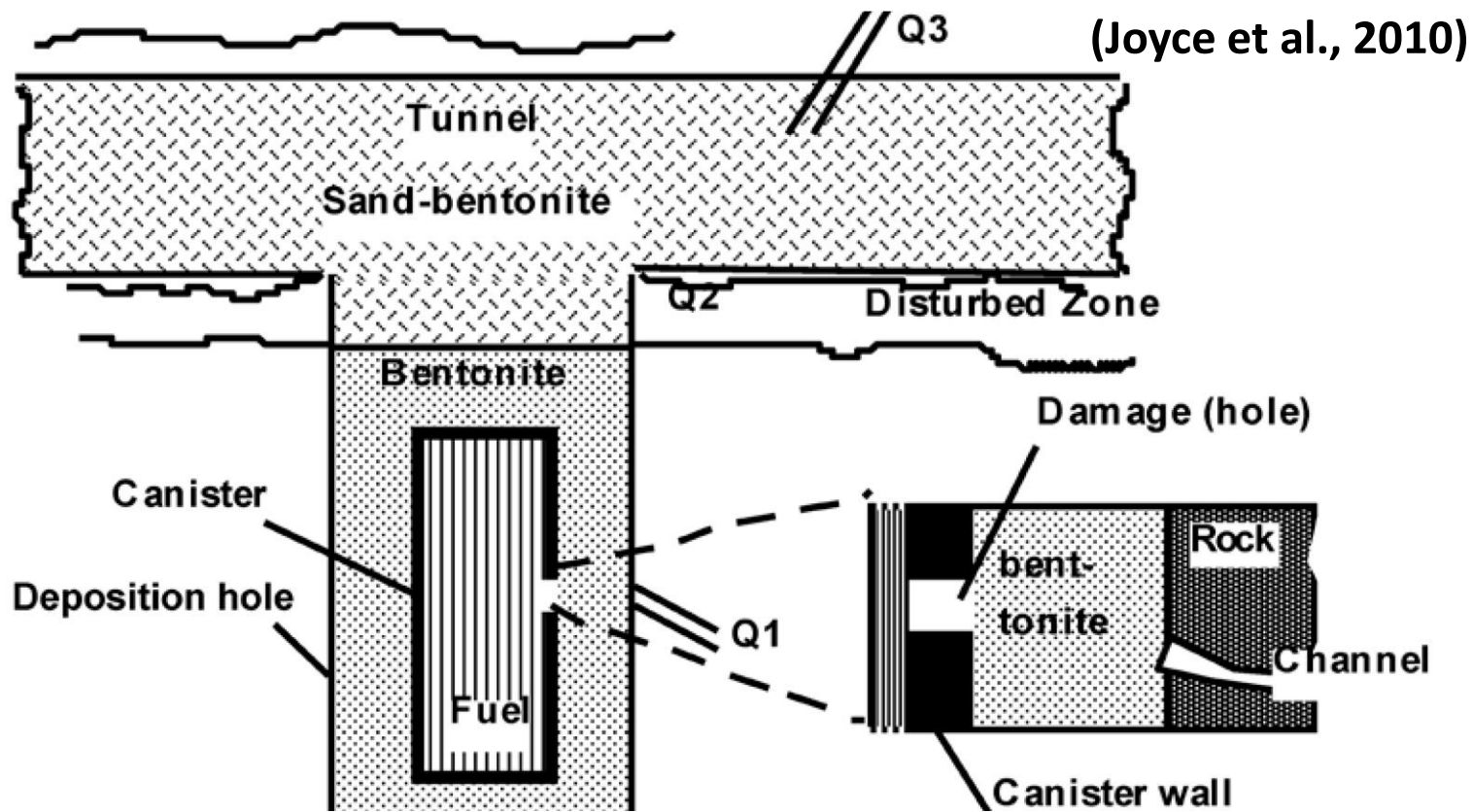
Thank you!

- ◆ Email: nichuenfa@geo.ncu.edu.tw
- ◆ Tel: +886-3-4227151 ext. 65874
- ◆ Fax: +886-3-4263127



國立中央大學 環境研究中心
Center for Environmental Studies





The solute encounters a number of transport resistances (Fr) in series. For example in the canister defect scenario for transport from the fuel to the seeping water a nuclide has to diffuse from the fuel through a hole in the canister to the clay buffer, then from the exit of the hole in the canister out into and through the buffer to reach the seeping water in the fracture in the rock. As the nuclide approaches the fracture in the rock it will have to find the narrow fracture. This can also be expressed as a resistance. All these resistances can be expressed as inverse of the corresponding equivalent flowrates.

volume of rock. This is a measure of the potential for retention and retardation of radionuclides within the rock.

The subscript “r” indicates that the PM is calculated in the rock. That is, they only represent cumulative PMs for those parts of paths within the rock and exclude parts of flow-paths that pass through the EDZ or tunnel backfill. PMs are calculated for legs of paths within the EDZ and tunnels, but are computed as separate PMs for each path and distinguish by an “EDZ” or “t” subscript, respectively.

In a DFN representation the PMs are defined as:

1. Travel-time, $t_r = \sum_f \frac{e_{fj} w_f \delta l}{Q_f}$, where δl is a step length along a path of f steps, each between

a pair of fracture intersections, e_{fj} is the fracture transport aperture, w_f is the flow width between the pair of intersections, and Q_f is the flow rate between the pair of intersections in the fracture.

2. Equivalent flux at the release point, U_r , described in more detail below.

3. Equivalent flow rate at the release point, Q_{eq} , described in more detail below.

4. Pathlength, $L_r = \sum_f \delta l$.

5. Flow-related transport resistance, $F_r = \sum_f \frac{2w_f \delta l}{Q_f} = \sum_f \frac{2t_{rf}}{e_{fj}}$, where t_{rf} is the travel time in a fracture along the path.

The results from the particle tracking are used to produce ensemble statistics for the performance measures, as well as locating the discharge areas. The ensemble is over the set of 8,031 particle start locations, one for each deposition hole and is in total divided over three blocks; block 1 with 2,158 start locations, block 2 with 3,576 start locations and block 3 with the remaining 2,297 start locations (Figure 3-13). Apart from the work done on the repository layout, no further attempt is made to avoid starting particles in either deterministic fracture zones or high transmissivity stochastic fractures. In reality, such features are likely to be avoided during repository construction, and hence the model may tend to see particles start in a wider range of possible fracture transmissivities than might be encountered in reality.

To avoid particles becoming stuck in regions of stagnant flow, they are not started if the initial flow rate per unit width is less than $1 \cdot 10^{-6}$ m²/y for Q1 and Q2 and the initial Darcy flux is less than $1 \cdot 10^{-6}$ m/y for Q3. For Q1 and Q2, flow rate per unit width, q_f , in a fracture is defined as

$$q_f = e_{fj} v = \frac{Q_f}{\sqrt{a_f}} \quad (3-6)$$

where:

- e_{fj} is the transport aperture of the fracture [m].
- v is the velocity [m/y].
- Q_f is the volumetric flow rate in the fracture [m³/y].
- a_f is the area of the fracture plane [m²].

For Q3, the Darcy flux, q , is defined as the volumetric flow rate per unit area.

Table 2-2. Summary of reported performance measures.

Performance measure	Description
t_r	Travel time in the rock [y].
U_r	Initial Darcy flux in the rock [m/y].
L_r	Path length in the rock [m].
F_r	Flow-related transport resistance in the rock [y/m].
t_t	Travel time in the tunnels [y].
U_t	Initial Darcy flux in the tunnels [m/y].
L_t	Path length in the tunnels [m].
t_{EDZ}	Travel time in the EDZ [y].
U_{EDZ}	Initial Darcy flux in the EDZ [m/y].
L_{EDZ}	Length in the EDZ [m].